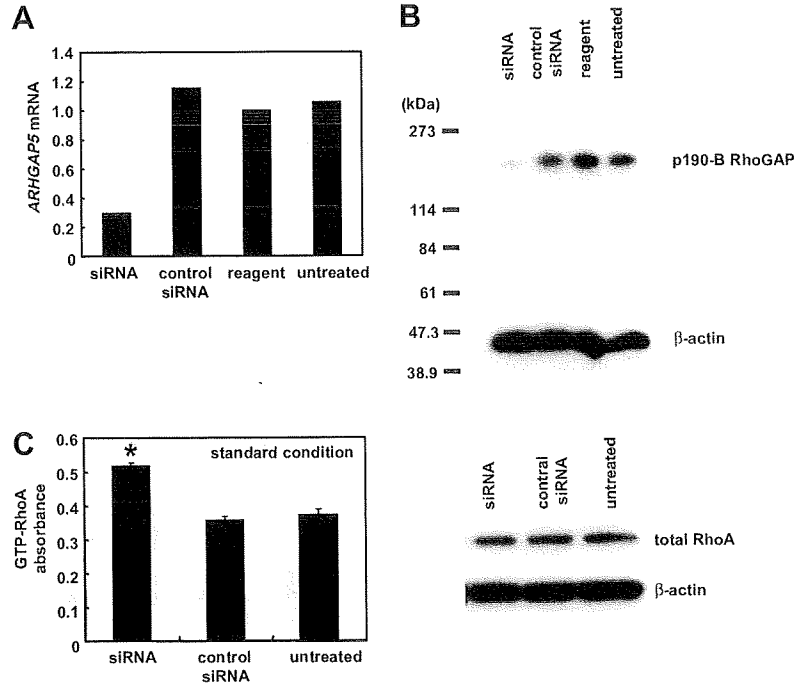

Fig. 3. Knockdown of *ARHGAP5* increases RhoA activity. (A) Relative expression levels of *ARHGAP5* mRNA as determined by real-time quantitative PCR. Huh-7 cells were treated with siRNA targeting *ARHGAP5*, negative control siRNA or transfection agent alone. Untreated cells were maintained under identical experimental conditions. Results are presented as a ratio between the expression level of *ARHGAP5* and that of a reference gene (*GAPDH*) to correct for variation in the amount of RNA. Relative expression levels were normalized such that the ratio in untreated cells was 1. (B) Levels of p190-B RhoGAP and β-actin, an internal control, determined by immunoblotting. (C) (*left*) Levels of RhoA activity under standard culture conditions (DMEM containing 10% FCS). RhoA activity was measured using a G-LISA kit (see Methods section). Values are represented as the mean ± S.D. Differences were analyzed by ANOVA ($^*P < 0.05$). (*right*) Total RhoA and β-actin were determined by immunoblotting.

3.3. Regulation of RhoA activity by p190-B RhoGAP in Huh-7 cells

To investigate the biological function of p190-B RhoGAP in HCC cells, knockdown of *ARHGAP5* expression in Huh-7 cells was carried out using RNAi. Following treatment of Huh-7 cells with siRNA targeting *ARHGAP5*, we observed a decrease in both *ARHGAP5* mRNA and p190-B RhoGAP protein levels relative to what was observed for cells receiving control siRNA, transfection agent alone or left untreated (Fig. 3A and B). Because p190-B RhoGAP negatively regulates RhoA activity, we examined the effect of the siRNA-mediated knockdown of *ARHGAP5* on RhoA activity. Huh-7 cells were treated with *ARHGAP5* siRNA or control siRNA or were left untreated. Cells were then cultured in DMEM containing 10% FCS for 48 h under standard conditions. RhoA activity levels were higher in cells treated with *ARHGAP5* siRNA than in cells treated with control siRNA or in untreated cells, whereas total RhoA levels were similar among the three groups (Fig. 3C). These findings suggest that overexpression of *ARHGAP5* contributes to downregulation of RhoA activity in Huh-7 cells.

3.4. Regulation of cell spreading by p190-B RhoGAP in Huh-7 cells

It is known that integrin-mediated adhesion regulates the activity of p190-B RhoGAP and RhoA [3,9]. We therefore examined the function of p190-B RhoGAP when Huh-7 cells were plated on fibronectin, a specific ligand for α5β1 integrin. Huh-7 cells treated with *ARHGAP5* siRNA or control siRNA or left untreated were suspended and plated on fibronectin. Prior to and during plating, cells were maintained in DMEM containing 1% FCS. Adhesion to fibronectin regulated RhoA activity in a triphasic or biphasic manner (Fig. 4A). Prior to plating (0 min), RhoA activity was significantly higher in *ARHGAP5* siRNA-treated cells than in control siRNA-treated cells or untreated cells. In *ARHGAP5* siRNA-treated cells, RhoA activity rapidly and transiently decreased (20 min). This initial decline was followed by an increase that peaked at 60 min. In the final phase, RhoA activity gradually decreased. In control siRNA-treated cells or untreated cells, an initial period of low RhoA activity was followed by a slight increase that peaked between 40–60 min and then returned to basal level. RhoA activity was significantly higher in *ARHGAP5* siRNA-treated cells than control siRNA-treated cells or untreated cells between 40 and 180 min. During the experimental period, expression of p190-B RhoGAP was continuously knocked down by *ARHGAP5* siRNA and total RhoA levels were similar among the three groups (Fig. 4A).

Because RhoA affects cell motility by stimulating reorganization of actin, we examined whether p190-B RhoGAP regulates the spreading of Huh-7 cells on fibronectin. Using immunofluorescence, we observed morphological changes in Huh-7 cells during attachment and spreading on fibronectin (Fig. 4B). Phalloidin staining revealed that *ARHGAP5* siRNA-treated cells exhibited more robust actin stress fibers but less membrane ruffling and protrusion at the cell periphery than control siRNA-treated cells or untreated cells. The actin stress fiber formation and reduced membrane ruffling and protrusion observed in *ARHGAP5* siRNA-treated cells corresponded with higher RhoA activity (Fig. 4)

p190-B RhoGAP was expressed diffusely in the cytoplasm of control siRNA-treated cells and untreated cells, whereas it was hardly detected in *ARHGAP5* siRNA-treated cells. We found that p190-B RhoGAP had partially translocated to the membrane protrusions in control siRNA-treated cells and untreated cells by 40 min after plating (Fig. 4B). Taken together, these findings suggest that RhoA inactivation by p190-B RhoGAP results in inhibition of actin stress fiber formation, enhanced membrane ruffling and protrusion and promotion of cell spreading on fibronectin.

3.5. Regulation of cell migration by p190-B RhoGAP in Huh-7 cells

To investigate the role of p190-B RhoGAP in cell motility, we performed a monolayer wound healing assay. Wound closure was delayed in *ARHGAP5* siRNA-treated cells relative to control siRNA-treated cells or untreated cells, whether cultured in the presence of mitomycin C or in its absence (Figs. 5A–E). Mitomycin C blocks mitosis and thus allows analysis of cell migration in the absence of cell proliferation. These results show that cell migration, rather than cell proliferation, is the major factor

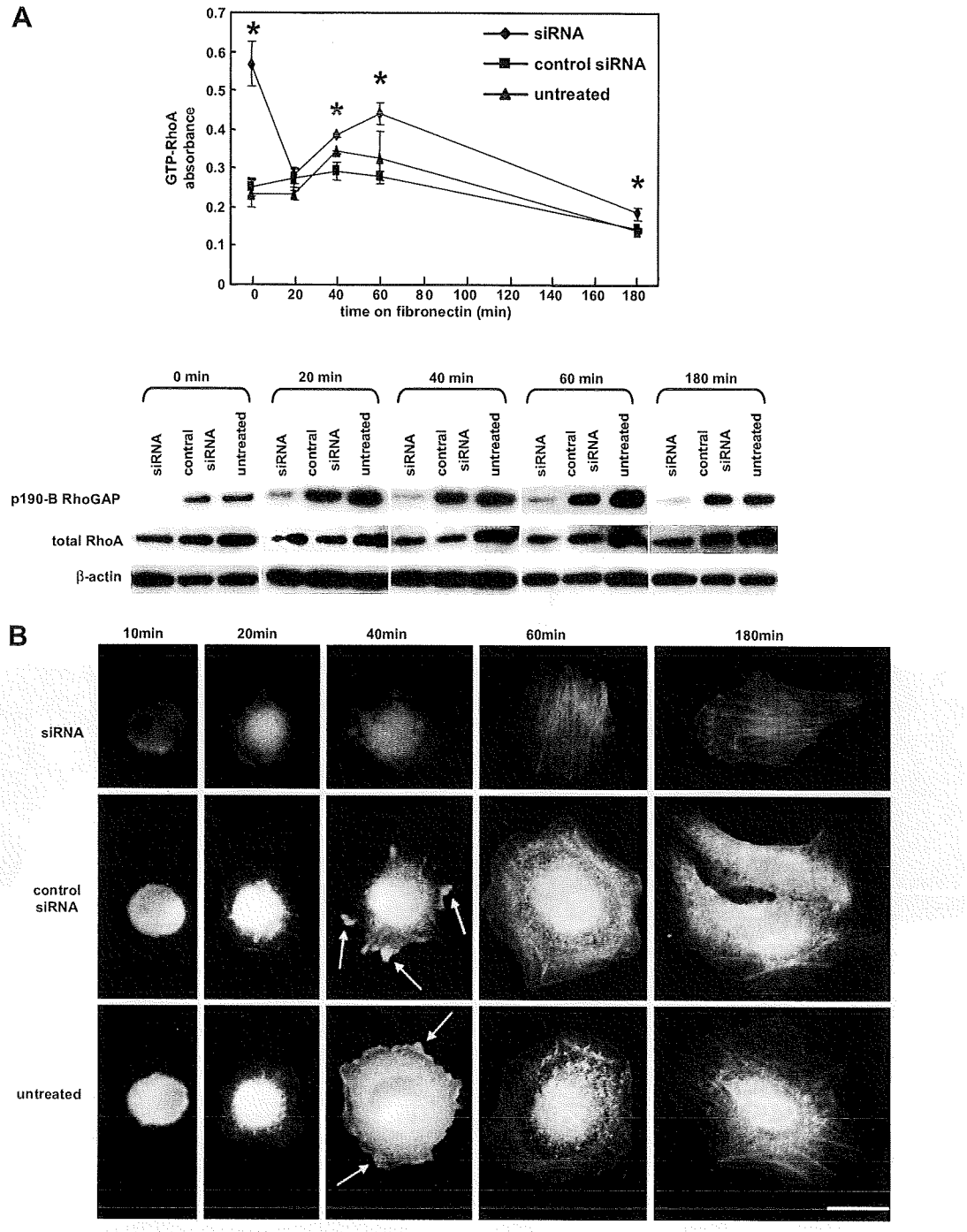

Fig. 4. Knockdown of *ARHGAP5* inhibits Huh-7 cell spreading on fibronectin. (A) Time course of changes in RhoA activity (*upper*) and levels of p190-B RhoGAP and total RhoA (*lower*). Huh-7 cells treated with siRNA targeting *ARHGAP5* or control siRNA or left untreated were plated on fibronectin as described in Materials and Methods and harvested at the indicated time points. Values of RhoA activity are represented as the mean ± SD. Differences were analyzed by ANOVA ($^{*}P < 0.05$). Levels of p190-B RhoGAP, total RhoA and β-actin were determined by immunoblotting. (B) Time course of cell spreading on fibronectin. Huh-7 cells treated with siRNA targeting *ARHGAP5* or control siRNA or left untreated were plated on fibronectin, fixed at the indicated time points and then triple-labeled with anti-p190-B RhoGAP, rhodamine-conjugated phalloidin and DAPI to reveal p190-B RhoGAP (green), actin filaments (red), and nuclei (blue), respectively. Arrows indicate p190-B RhoGAP on membrane protrusions. Scale bar = 10 μm.

in the retarded wound repair process in *ARHGAP5* siRNA-treated cells. Wound edge cells in *ARHGAP5* siRNA-treated cells had more abundant actin stress fibers but less membrane ruffling and protrusion at the leading edge than control siRNA-treated or untreated cells (Figs. 5F–H). p190-B RhoGAP translocated to the membrane protrusions of control siRNA-treated or untreated cells at the edge of the wound, but not in *ARHGAP5*-siR-

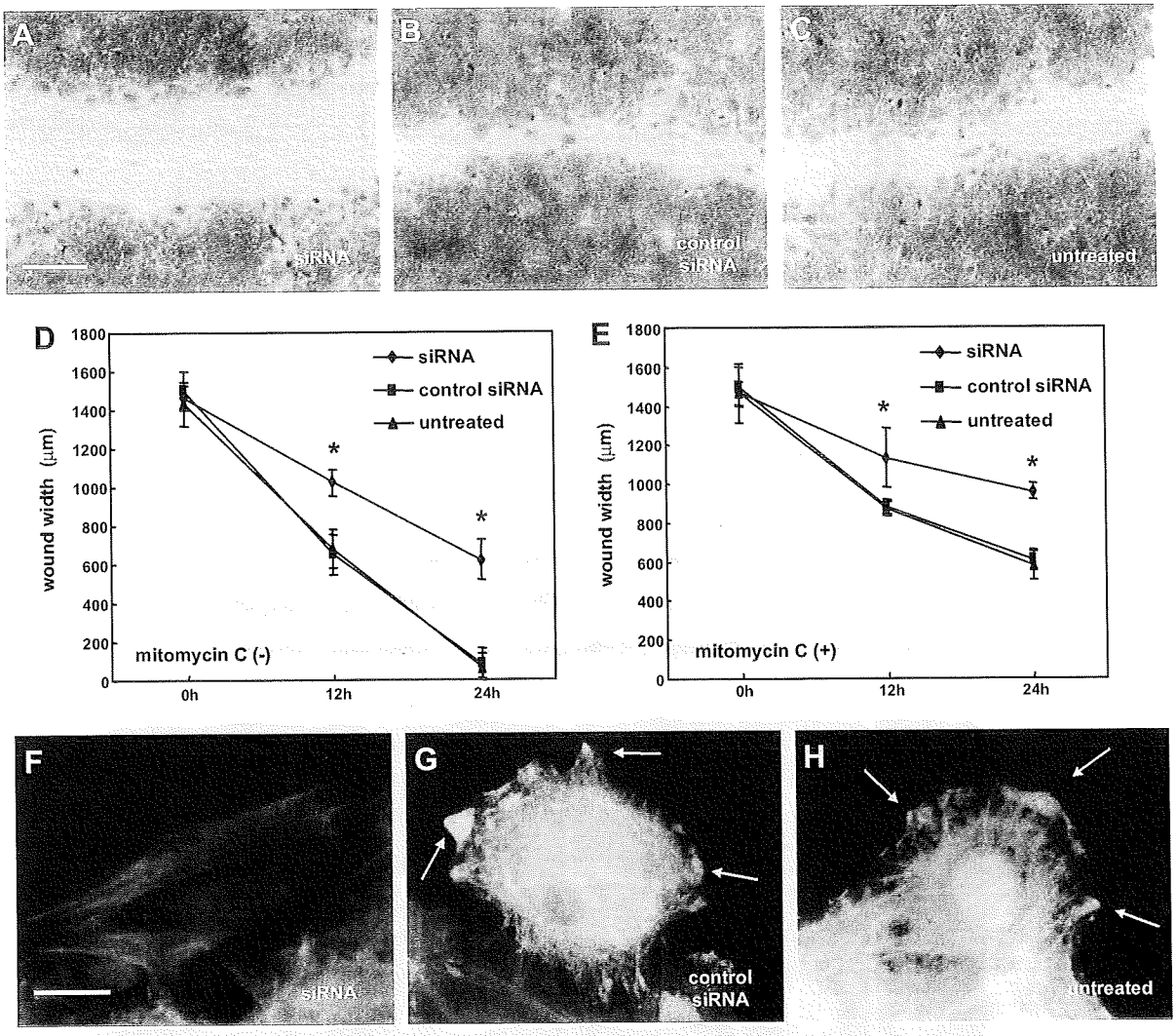

Fig. 5. Knockdown of *ARHGAP5* inhibits migration in Huh-7 cells. Monolayer wound healing assay in Huh-7 cells transfected with siRNA targeting *ARHGAP5* (A, F) or control siRNA (B and G), or left untreated (C and H). Cells were cultured in the absence (A–D, F–H) or presence (E) of mitomycin C. (A–C) Cells were allowed to migrate into a monolayer wound for 24 h and afterward stained with Giemsa stain. Original magnifications: 40×. Scale bar = 500 μm. (D and E) Cells were cultured in the absence (D) or presence (E) of mitomycin C. Wound widths were measured in three randomly chosen regions at the indicated time after wounding. Values are represented as the mean ± SD. Differences were analyzed by ANOVA ($^{*}P < 0.05$). (F–H) Wound edge cells were triple-labeled with anti-p190-B RhoGAP, rhodamine-conjugated phalloidin and DAPI to reveal p190-B RhoGAP (green), actin filaments (red) and nuclei (blue), respectively. Arrows indicate p190-B RhoGAP on membrane protrusions. Scale bar = 10 μm.

NA cells. Taken together, these observations suggest that the inhibition of RhoA activity by p190-B RhoGAP promotes cell movement and formation of membrane protrusions in migrating cells.

4. Discussion

We report here the amplification of *ARHGAP5* in HCC and ESCC cell lines. We undertook a molecular definition of the amplicon at 14q12 that is present in HCC and ESCC cell lines. The amplification at 14q12 has been reported in various types of cancers, including HCC [10], ESCC [7], nasopharyngeal carcinoma [11] and non-squamous cell lung carcinoma [12], although the frequency of 14q12 gain is low in primary HCC (4–6%) [10,13]. The range of the amplicon varies among these tumors, and their boundaries have not been determined in each case. Moreover, the target oncogene(s) in the amplified regions have not been fully identified. Here we defined the amplified regions in one HCC and two ESCC cell lines and narrowed the site of the amplification to a relatively short section. Among the four genes within the smallest region of the amplification, only *HEATR5A* and *ARHGAP5* were overexpressed in all the tested lines exhibiting copy number gains in the region; hence they are thought to be candidate targets in the amplicon. Of the two genes, we chose to focus further analysis on *ARHGAP5* because its protein product, p190-B RhoGAP, is purported to play an important role in dynamic cellular processes by regulating RhoA activity, while little is known about *HEATR5A*. During the preparation of this manuscript, amplification of *ARHGAP5* was reported in Huh-7 cells [14].

Although several studies have suggested an association of p190-B RhoGAP with tumors [15–17], its biological function in cancer cells is poorly understood. Therefore, using siRNA, we studied its function in Huh-7 cells, the HCC cell line that exhibited the most remarkable copy number gain and overexpression of *ARHGAP5*. We found that p190-B RhoGAP negatively regulates RhoA activity in Huh-7 cells cultured in medium containing 10% FCS and plated on fibronectin. Adhesion to fibronectin regulated RhoA activity in a triphasic or biphasic manner, as previously reported in fibroblasts [18,19]. Although some RhoA activity is required for migration, possibly to maintain sufficient adhesion to the substrate, high activity inhibits movement [19–22]. Our results showed that RhoA inactivation by p190-B RhoGAP results in inhibition of actin stress fiber formation, enhanced membrane ruffling and protrusion, and promotion of spreading and migration of Huh-7 cells. These findings are in agreement with results obtained from previous studies. A dominant negative (loss-of-function) p190-B RhoGAP mutation elevates RhoA activity in fibroblasts cultured on fibronectin and inhibits their migration, whereas overexpression of wild-type p190-B RhoGAP decreases RhoA activity, promotes the formation of membrane protrusions and enhances mobility [19]. Activation of β1 integrin signaling stimulates tyrosine phosphorylation of p190-B RhoGAP and promotes membrane protrusion at invadopodia in a melanoma cell line [17]. p190-B RhoGAP is also involved in invasion by breast cancer cells [15].

In conclusion, we have identified *ARHGAP5* as a probable target for the amplification at 14q12 detected in a subgroup of HCCs and ESCCs. Our results indicate that p190-B RhoGAP, the protein product of *ARHGAP5*, promotes cell spreading and migration in Huh-7 cells. Further studies are needed to determine the importance of *ARHGAP5* and p190-B RhoGAP in the development and progression of not only HCC and ESCC but also other types of tumors.

Conflicts of interest statement

My co-authors and I declare that we have no proprietary, financial, professional or other personal interest of any nature or kind in any product, service and/or company that could be construed as influencing the position presented in the manuscript entitled, "A novel amplification target, ARHGAP5, promotes cell spreading and migration by negatively regulating RhoA in Huh-7 hepatocellular carcinoma cells".

Acknowledgements

Supported by: Grants-in-Aid for Scientific Research (18390223) from the Japan Society for the Program of Science (to K.Yasui).

References

[1] A. Hall, Rho GTPases and the actin cytoskeleton, Science 279 (1998) 509–514.
[2] P.D. Burbelo, S. Miyamoto, A. Utani, S. Brill, K.M. Yamada, A. Hall, Y. Yamada, P190-B, a new member of the Rho GAP family, and Rho are induced to cluster after integrin cross-linking, J. Biol. Chem. 270 (1995) 30919–30926.
[3] W.T. Arthur, L.A. Petch, K. Burridge, Integrin engagement suppresses RhoA activity via a c-Src-dependent mechanism, Curr. Biol. 10 (2000) 719–722.
[4] G.C. Kennedy, H. Matsuzaki, S. Dong, W.N. Liu, J. Huang, G. Liu, X. Su, M. Cao, W. Chen, J. Zhang, W. Liu, G. Yang, X. Di, T. Ryder, Z. He, U. Surti, M.S. Phillips, M.T. Boyce-Jacino, S.P. Fodor, K.W. Jones, Large-scale genotyping of complex DNA, Nat. Biotechnol. 21 (2003) 1233–1237.
[5] Y. Nannya, M. Sanada, K. Nakazaki, N. Hosoya, L. Wang, A. Hangaishi, M. Kurokawa, S. Chiba, D.K. Bailey, G.C. Kennedy, S. Ogawa, A robust algorithm for copy number detection using high-density oligonucleotide single nucleotide polymorphism genotyping arrays, Cancer Res. 65 (2005) 6071–6079.
[6] Y. Inagaki, K. Yasui, M. Endo, T. Nakajima, K. Zen, K. Tsuji, M. Minami, S. Tanaka, M. Taniwaki, Y. Itoh, S. Arii, T. Okanoue, CREB3L4, INTS3, and SNAPAP are targets for the 1q21 amplicon frequently detected in hepatocellular carcinoma, Cancer Genet. Cytogenet. 180 (2008) 30–36.
[7] K. Yasui, I. Imoto, Y. Fukuda, A. Pimkhaokham, Z.Q. Yang, T. Naruto, Y. Shimada, Y. Nakamura, J. Inazawa, Identification of target genes within an amplicon at 14q12–q13 in esophageal squamous cell carcinoma, Genes Chromosomes Cancer 32 (2001) 112–118.
[8] C. Collins, J.M. Rommens, D. Kowbel, T. Godfrey, M. Tanner, S.I. Hwang, D. Polikoff, G. Nonet, J. Cochran, K. Myambo, K.E. Jay, J. Froula, T. Cloutier, W.L. Kuo, P. Yaswen, S. Dairkee, J. Giovanola, G.B. Hutchinson, J. Isola, O.P. Kallioniemi, M. Palazzolo, C. Martin, C. Ericsson, D. Pinkel, D. Albertson, W.B. Li, J.W. Gray, Positional cloning of ZNF217 and NABC1: genes amplified at 20q13.2 and overexpressed in breast carcinoma, Proc. Natl. Acad. Sci. USA 95 (1998) 8703–8708.
[9] E.A. Cox, S.K. Sastry, A. Huttenlocher, Integrin-mediated adhesion regulates cell polarity and membrane protrusion through the Rho family of GTPases, Mol. Biol. Cell 12 (2001) 265–277.
[10] C. Sakakura, A. Hagiwara, H. Taniguchi, T. Yamaguchi, H. Yamagishi, T. Takahashi, K. Koyama, Y. Nakamura, T. Abe, J. Inazawa, Chromosomal aberrations in human hepatocellular carcinomas associated with hepatitis C virus infection detected by comparative genomic hybridization, Br. J. Cancer 80 (1999) 2034–2039.
[11] Y.J. Chen, J.Y. Ko, P.J. Chen, C.H. Shu, M.T. Hsu, S.F. Tsai, C.H. Lin, Chromosomal aberrations in nasopharyngeal carcinoma analyzed by comparative genomic hybridization, Genes Chromosomes Cancer 25 (1999) 169–175.
[12] T. Yakut, H.J. Schulten, A. Demir, D. Frank, B. Danner, U. Egeli, C. Gebitekin, E. Kahler, B. Gunawan, N. Urer, H. Oztürk, L. Füzesi, Assessment of molecular events in squamous and non-squamous cell lung carcinoma, Lung Cancer 54 (2006) 293–301.
[13] P. Moinzadeh, K. Breuhahn, H. Stützer, P. Schirmacher, Chromosome alterations in human hepatocellular carcinomas correlate with aetiology and histological grade – results of an explorative CGH meta-analysis, Br. J. Cancer 92 (2005) 935–941.
[14] C. Schlaeger, T. Longerich, C. Schiller, P. Bewerunge, A. Mehrabi, G. Toedt, J. Kleeff, V. Ehemann, R. Eils, P. Lichter, P. Schirmacher, B. Radlwimmer, Etiology-dependent molecular mechanisms in human hepatocarcinogenesis, Hepatology 47 (2008) 511–520.
[15] S. Zrihan-Licht, Y. Fu, J. Settleman, K. Schinkmann, L. Shaw, I. Keydar, S. Avraham, H. Avraham, RAFTK/Pyk2 tyrosine kinase mediates the association of p190 RhoGAP with RasGAP and is involved in breast cancer cell invasion, Oncogene 19 (2000) 1318–1328.
[16] G. Chakravarty, D. Roy, M. Gonzales, J. Gay, A. Contreras, J.M. Rosen, P190-B, a Rho-GTPase-activating protein, is differentially expressed in terminal end buds and breast cancer, Cell Growth Differ. 11 (2000) 343–354.
[17] H. Nakahara, S.C. Mueller, M. Nomizu, Y. Yamada, Y. Yeh, W.T. Chen, Activation of beta1 integrin signaling stimulates tyrosine phosphorylation of p190RhoGAP and membrane-protrusive activities at invadopodia, J. Biol. Chem. 273 (1998) 9–12.
[18] X.D. Ren, W.B. Kiosses, M.A. Schwartz, Regulation of the small GTP-binding protein Rho by cell adhesion and the cytoskeleton, EMBO J. 18 (1999) 578–585.
[19] W.T. Arthur, K. Burridge, RhoA inactivation by p190RhoGAP regulates cell spreading and migration by promoting membrane protrusion and polarity, Mol. Biol. Cell 12 (2001) 2711–2720.
[20] K. Takaishi, T. Sasaki, M. Kato, W. Yamochi, S. Kuroda, T. Nakamura, M. Takeichi, Y. Takai, Involvement of Rho p21 small GTP-binding protein and its regulator in the HGF-induced cell motility, Oncogene 9 (1994) 273–279.
[21] A.J. Ridley, P.M. Comoglio, A. Hall, Regulation of scatter factor/hepatocyte growth factor responses by Ras, Rac, and Rho in MDCK cells, Mol. Cell. Biol. 15 (1995) 1110–1122.
[22] C.D. Nobes, A. Hall, Rho GTPases control polarity, protrusion, and adhesion during cell movement, J. Cell Biol. 144 (1999) 1235–1244.

Hepatol Int (2009) 3:445–452
DOI 10.1007/s12072-009-9135-0

ORIGINAL ARTICLE

Antiviral activity, dose–response relationship, and safety of entecavir following 24-week oral dosing in nucleoside-naive Japanese adult patients with chronic hepatitis B: a randomized, double-blind, phase II clinical trial

Michiko Shindo · Kazuaki Chayama · Satoshi Mochida · Joji Toyota · Eiichi Tomita · Hiromitsu Kumada · Osamu Yokosuka · Michio Sata · Norio Hayashi · Kazuyuki Suzuki · Takeshi Okanoue · Hirohito Tsubouchi · Hiroki Ishikawa · Taku Seriu · Masao Omata

Received: 21 January 2009 / Accepted: 7 May 2009 / Published online: 23 May 2009

Abstract
Purpose A randomized, double-blind, multicenter study (ETV-047) was conducted to evaluate the dose–response relationship of entecavir and compare its antiviral activity and safety with lamivudine in Japanese patients with chronic hepatitis B (CHB).
Methods One hundred thirty-seven nucleoside-naive adult patients with CHB were randomized to once-daily oral doses of entecavir 0.01, 0.1, or 0.5 mg or lamivudine 100 mg for 24 weeks. The primary efficacy end point used to evaluate the dose–response relationship was mean change from baseline in serum hepatitis B virus (HBV) DNA level at week 22, as determined by polymerase chain reaction assay.
Results Entecavir demonstrated a clear dose–response relationship, with mean change from baseline in serum

M. Shindo (✉)
Division of Liver Disease, Department of Internal Medicine, Akashi Municipal Hospital, 1-33 Takasyo-machi, Akashi-shi, Hyogo, Japan
e-mail: mshindo@skyblue.ocn.ne.jp

K. Chayama
Department of Medicine and Molecular Science, Graduate School of Biomedical Sciences, Hiroshima University, Hiroshima, Japan

S. Mochida
Department of Gastroenterology and Hepatology, Saitama Medical University, Saitama, Japan

J. Toyota
Department of Hepatology, Sapporo Kosei General Hospital, Hokkaido, Japan

E. Tomita
Department of Gastroenterology, Gifu Municipal Hospital, Gifu, Japan

H. Kumada
Department of Hepatology, Toranomon Hospital, Tokyo, Japan

O. Yokosuka
Department of Medicine and Clinical Oncology, Graduate School of Medicine, Chiba University, Chiba, Japan

M. Sata
Department of Gastroenterology, Kurume University School of Medicine, Fukuoka, Japan

N. Hayashi
Department of Gastroenterology and Hepatology, Osaka University Graduate School of Medicine, Osaka, Japan

K. Suzuki
Department of Internal Medicine, Iwate Medical University, Iwate, Japan

T. Okanoue
Department of Gastroenterology, Saiseikai Suita Hospital, Osaka, Japan

H. Tsubouchi
Department of Digestive Disease and Lifestyle-Related Disease, Kagoshima University Graduate School of Medical and Dental Sciences, Kagoshima, Japan

H. Ishikawa · T. Seriu
Pharmaceutical Research Institute, Bristol-Myers Squibb Japan, Tokyo, Japan

M. Omata
Department of Gastroenterology, Graduate School of Medicine, University of Tokyo, Tokyo, Japan

HBV DNA level of −3.11, −4.77, and −5.16 $\log_{10}$ copies/ml with entecavir 0.01, 0.1, and 0.5 mg, respectively. Entecavir 0.5 mg was superior to lamivudine 100 mg for the mean change in HBV DNA level (−5.16 vs. −4.29 $\log_{10}$ copies/ml; $P = 0.007$). The overall incidence of adverse events was comparable between treatment groups. Two patients discontinued treatment because of adverse events (one with liver cirrhosis [entecavir 0.5 mg] and one with grade 4 serum alanine aminotransferase (ALT) elevation, nausea, and malaise [lamivudine 100 mg]). Serum ALT flares were observed in four patients; flares were associated with 2 $\log_{10}$ reductions or more in HBV DNA level and resolved without dose interruption.

Conclusion Entecavir 0.01–0.5 mg is well tolerated and produces a dose-dependent reduction in viral load in nucleoside-naive Japanese patients with CHB. Compared with lamivudine 100 mg, entecavir 0.1 mg demonstrated noninferiority and entecavir 0.5 mg was superior in this population.

Keywords Chronic hepatitis B · Entecavir · Lamivudine · HBV DNA · ALT flare

Introduction

It is reported that more than 2 billion individuals worldwide have been infected with hepatitis B virus (HBV) and approximately 350 million people are long-term HBV carriers [1]. Chronic hepatitis B (CHB) is induced by chronic replication of HBV in the liver and has a poor prognosis, with 20–40% of infected individuals developing liver cirrhosis, noncompensated liver disorder, or hepatocellular carcinoma [2]. Treatment of CHB is aimed at sustained inhibition of HBV replication and remission of liver disease [3], ultimately preventing progression to liver cirrhosis or hepatocellular carcinoma [4].

Prior to the advent of the nucleoside analog lamivudine, interferon-α formed the mainstay of treatment, but this immunoregulatory cytokine requires parenteral administration and is poorly tolerated [5]. Lamivudine is well tolerated on oral administration and has been proven to be highly effective in the treatment of CHB, but the emergence of resistance mutations (including the YMDD motif) in the reverse-transcriptase domain of HBV polymerase frequently results in overt viral rebound and disease progression [6–9]. The novel nucleoside analog adefovir is effective against wild-type HBV and lamivudine-resistant strains and is well tolerated on long-term administration, but its clinical use is restricted by the need for renal monitoring in patients with impaired renal function [10].

Entecavir, a cyclopentylguanine-derived nucleoside analog and selective inhibitor of HBV replication, was approved by the U.S. Food and Drug Administration in 2005 for the treatment of CHB. Entecavir displays potent antiviral activity in the woodchuck and duck models of HBV infection [11, 12] and is reported to be 100- to 2,200-fold more potent than lamivudine and adefovir in inhibiting HBV replication in vitro [13, 14]. Phase II clinical trials of entecavir conducted in non-Japanese patients with CHB have demonstrated entecavir to be well tolerated and more effective than lamivudine [15, 16].

A global dose-finding study (ETV-005) conducted in lamivudine-naive patients with CHB compared three doses of entecavir (0.01, 0.1, and 0.5 mg once daily) with lamivudine 100 mg once daily over a 22-week treatment period. Entecavir showed a clear dose–response relationship and was well tolerated at all three dose levels; in addition, 0.1 and 0.5 mg of entecavir showed superior antiviral activity compared with 100 mg of lamivudine [15].

Phase I studies of single-dose (0.05–2.5 mg) and multiple-dose (0.1–1.0 mg daily) entecavir conducted in Japan have confirmed the drug's safety in healthy men. As in Caucasian populations, entecavir displayed linear plasma pharmacokinetics over a wide range of doses, including putative therapeutic doses (0.5 and 1.0 mg), in Japanese subjects; there was no evidence of significant ethnic differences in its pharmacokinetics and pharmacodynamics. Similar findings to those obtained in the global phase II clinical trials of entecavir might therefore be expected from corresponding studies conducted in Japanese patients.

To evaluate the dose–response relationship, the antiviral activity and safety of entecavir in Japanese CHB patients, we conducted a 24-week phase II study comparing entecavir (0.01, 0.1, and 0.5 mg daily) to lamivudine (100 mg daily).

Materials and methods

Study design

This randomized, double-blind, double-dummy study was conducted at 38 institutions in Japan from August 2003 to March 2005. Eligible patients comprised 20- to 75-year-old men and women with CHB who fulfilled the following criteria: (i) HBsAg-positive for 24 weeks or more or IgM HBcAb-negative with biopsy-confirmed CHB; (ii) HBeAg-positive or HBeAg-negative for 12 weeks or more; (iii) serum HBV DNA level 40 MEq/ml or more (143 pg/ml) by Quantiplex™ branched DNA hybridization method (bDNA assay) (≥7.6 $\log_{10}$ genome equivalent by the transcription-mediated amplification method or $\geq 10^{7.6}$ copies/ml by Roche Amplicor™ polymerase chain reaction method [PCR assay]) measured 2 weeks or more before screening and serum HBV DNA level 40 MEq/ml or more (by bDNA assay) at screening; (iv) serum alanine

aminotransferase (ALT) level 1.25–10 times the upper limit of normal (ULN); and (v) well-compensated liver disease with prothrombin time prolongation 3 s or less or international normalized ratio 1.5 or less, serum albumin level 3.0 g/dl or more, and total bilirubin 2.5 mg/dl or less (42.75 μmol/l). After a 6-week screening period, eligible patients were stratified according to HBeAg status and study site and randomized (1:1:1:1) to oral treatment with entecavir (0.01, 0.1, or 0.5 mg plus matching placebo capsule) or lamivudine (100 mg plus matching placebo tablet) once daily for 24 weeks. All doses were administered at fixed times of the day, avoiding the 2 h before and after meals. Pregnant women were excluded from the study, as were patients with liver cirrhosis, patients with a history or evidence of variceal bleeding, patients with hepatic encephalopathy or ascites requiring diuretics, or patients with paracentesis. Patients with other liver disease (e.g., autoimmune hepatitis) were excluded from the study. In addition, patients were excluded if they had a serum creatinine level more than 1.5 × ULN, hemoglobin level less than 10.0 g/dl, platelet count less than 70,000/mm^3, granulocyte count less than <1,500/mm^3 or plasma α-fetoprotein level more than 100 ng/ml, a history of allergy induced by nucleoside analog or exposure to nucleoside analogs, a recent history (previous 24 weeks) of treatment with immunosuppressives or interferon-α/β, or current treatment of CHB.

Treatment efficacy was assessed after 22 weeks, and all eligible patients who completed 24 weeks of blinded therapy were given the option of enrolling in a separate entecavir trial. Patients who discontinued therapy prematurely were followed up for 24 weeks postdosing. Patients began anti-HBV therapy as recommended by their physician during the postdosing follow-up period.

Informed consent was obtained from all patients in writing prior to their inclusion in the study. The study was conducted in accordance with the principles of the Declaration of Helsinki and Good Clinical Practice guidelines and notifications were issued by the Ministry of Health and Labor.

Efficacy and safety assessment

The primary efficacy end point for the evaluation of the dose–response relationship of entecavir was the change from baseline in mean serum HBV DNA level at week 22, as determined by PCR assay. Secondary efficacy end points for the assessment of the noninferiority of entecavir at each dose to lamivudine included the change from baseline in mean serum HBV DNA level at week 22, as determined by PCR assay, the percentage of patients with a reduction in serum HBV DNA level 2 $\log_{10}$ copies/ml or more or a serum HBV DNA level below the limit of detection (400 copies/ml by PCR assay; 2.5 pg/ml or 0.7 MEq/ml by bDNA assay) at week 22, the percentage of patients with HBeAg loss, the percentage of patients with HBeAg seroconversion (HBeAg loss and appearance of HBe-antibody), the percentage of patients achieving ALT normalization (World Health Organization grade 0: <1.25 × ULN), and the percentage of patients achieving a protocol-defined response (HBV DNA level <0.7 MEq/ml by bDNA assay, HBeAg negativity and serum ALT level <1.25 × ULN for HBeAg-positive patients; HBV DNA level <0.7 MEq/ml by bDNA assay and serum ALT level <1.25 ULN for HBeAg-negative patients) at week 22. The incidence of genotypic drug resistance was also assessed in patients who had a 1 $\log_{10}$ copies/ml or more increase in HBV DNA by PCR from nadir while on study drug.

Based on the results of the global dose–response study of entecavir conducted in nucleoside-naive patients (ETV-005 study) [15], noninferiority of entecavir 0.1 or 0.5 mg compared with lamivudine (100 mg) was confirmed if the upper 95% confidence interval (CI) for the difference in mean HBV DNA levels at week 22 was 0.8 $\log_{10}$ copies/ml or less.

Assay methods

Serum HBV DNA level was determined by Roche Amplicor™ PCR assay (Roche Diagnostics K.K., Tokyo, Japan) and Quantiplex™ (Chiron) bDNA assay. Clinical laboratory tests, serum HBV DNA assays, and HBV serology were performed at the central clinical laboratory designated by the trial sponsor. Genotypic analysis of HBV isolates was performed using samples collected from patients on the first day of treatment. Genotypic analysis of HBV DNA polymerase was performed at SRL Inc. (Tokyo, Japan).

Statistical analysis

Numerical data were expressed by descriptive statistics. Serum HBV DNA level, a continuous variable, was analyzed after logarithmic transformation. For treatment group, comparisons of continuous variables, analysis of variance models, incorporating baseline HBV DNA level and HBeAg status as covariates were employed. For intertreatment comparisons of binary data, Cochran–Mantel–Haenszel tests were employed using baseline HBeAg status as a stratification factor. For analysis of dose–response relationships, Student's t test was applied to linear regression plots of serum HBV DNA level against log dose. A two-sided $P < 0.05$ was taken to indicate statistical significance. For analysis of dose–response relationships using efficacy data, a two-sided $P < 0.05/3$ was taken to

indicate statistical significance following Bonferroni adjustment.

Results

Study population and demographic characteristics

A total of 137 patients, including 20- to 73-year-old men and women, met the study eligibility criteria and were randomized to the following treatment groups: entecavir 0.01 mg ($n = 35$), entecavir 0.1 mg ($n = 34$), entecavir 0.5 mg ($n = 34$), and lamivudine 100 mg ($n = 34$). Three patients (two in the entecavir 0.5 mg group and one in the lamivudine 100 mg group) discontinued the study prematurely; the reasons for discontinuation were noncompliance (one patient in the entecavir 0.5 mg group) and adverse events (liver cirrhosis in one patient [entecavir 0.5 mg group] and grade 4 serum ALT elevation with nausea and malaise in one patient [lamivudine 100 mg group]). Accordingly, a total of 134 patients (entecavir 0.01 mg group, 35 patients; entecavir 0.1 mg group, 34 patients; entecavir 0.5 mg group, 32 patients; and lamivudine 100 mg group, 33 patients) completed 24 weeks of treatment and were included in the efficacy assessment.

The four treatment groups were matched with respect to gender, age, body weight, and proportion of HBeAg-positive patients (Table 1). Serum HBV DNA levels by PCR assay (mean ± SD) at baseline were 7.94 ± 0.87, 8.09 ± 1.05, 8.39 ± 0.73, and 7.94 ± 0.83 $\log_{10}$ copies/ml for the entecavir 0.01, 0.1, and 0.5 mg and lamivudine 100 mg groups, respectively. With regard to HBV genotype, 124 patients were genotype C, 6 patients were genotype A, 5 patients were genotype B, and 2 patients were genotype F. All patients were nucleos(t)ide-naive and none had been pretreated with interferon therapy.

Virologic response

Mean changes (from baseline) in serum HBV DNA level at week 22 were −3.11, −4.77, and −5.16 $\log_{10}$ copies/ml with entecavir 0.01, 0.1, and 0.5 mg, respectively (Fig 1; Table 2). Estimated differences in serum HBV DNA levels between the 0.1 and 0.5 mg entecavir groups and the low-dose entecavir group (0.01 mg) were determined after adjustment for baseline level and HBeAg status. Estimated intertreatment group differences (adjusted 95% CI) were −1.61 (−2.20 to −1.02) $\log_{10}$ copies/ml between the entecavir 0.01 and 0.1 mg groups and −1.95 (−2.53 to −1.37) $\log_{10}$ copies/ml between the entecavir 0.5 and 0.01 mg groups; both of these differences were statistically significant ($P < 0.0001$). In contrast, the difference in serum HBV DNA levels between the high-dose (0.5 mg) and medium-dose (0.1 mg) entecavir groups was not statistically significant (estimated difference [adjusted 95% CI] −0.23 [−0.69 to 0.23] $\log_{10}$ copies/ml). Taken together, these results demonstrate the superiority of high- and medium-dose entecavir (0.1 and 0.5 mg) compared with low-dose entecavir (0.01 mg) in terms of viral load reduction (Table 3). Linear regression analyses indicated a

Table 1 Baseline demographics and clinical characteristics of treated subjects

	ETV 0.01 mg ($n = 35$)	ETV 0.1 mg ($n = 34$)	ETV 0.5 mg ($n = 34$)	LVD 100 mg ($n = 34$)
Male, *n* (%)	25 (71.4)	23 (67.6)	23 (67.6)	28 (82.4)
Female, *n* (%)	10 (28.6)	11 (32.4)	11 (32.4)	6 (17.6)
Age (years), mean ± SD	42.0 ± 12.5	40.1 ± 9.8	39.8 ± 10.4	42.3 ± 12.6
Weight (kg), mean ± SD	66.2 ± 12.5	64.6 ± 11.9	65.3 ± 11.1	64.4 ± 9.0
Ethnicity Japanese, *n* (%)	35 (100)	34 (100)	34 (100)	34 (100)
HBV DNA ($\log_{10}$ copies/ml by PCR), mean ± SD	7.94 ± 0.87	8.09 ± 1.05	8.39 ± 0.73	7.94 ± 0.83
HBeAg positive, *n* (%)	30 (85.7)	30 (88.2)	30 (88.2)	31 (91.2)
ALT (IU/l), mean ± SD	150.1 ± 111.8	162.0 ± 127.1	142.4 ± 82.2	185.0 ± 130.8
AST (IU/l), mean ± SD	83.2 ± 40.0	114.3 ± 109.4	81.0 ± 43.0	121.6 ± 85.4
Total bilirubin (mg/dl), mean ± SD	0.65 ± 0.25	0.56 ± 0.15	0.66 ± 0.25	0.71 ± 0.28
HBV genotype (%)				
C	32 (91.4)	30 (88.2)	32 (94.1)	30 (88.2)
A	1 (2.86)	2 (5.88)	1 (2.94)	2 (5.88)
B	1 (2.86)	1 (2.94)	1 (2.94)	2 (5.88)
F	1 (2.86)	1 (2.94)	0	0

ETV entecavir; *LVD* lamivudine

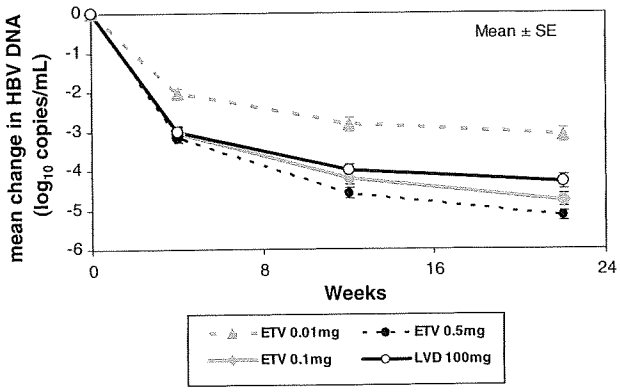

Fig. 1 Mean change from baseline in serum HBV DNA level by PCR assay through 22 weeks in patients treated with entecavir (ETV) 0.01, 0.1, and 0.5 mg and lamivudine 100 mg. Mean change in serum HBV DNA level was plotted as a function of time after the initiation of the protocol therapy (weeks). Data expressed as mean ± SE

significant dose–response relationship between $\log_{10}$ entecavir dose and reduction in $\log_{10}$ serum HBV DNA level ($P < 0.0001$).

Mean change (from baseline) in serum HBV DNA level at week 22 for the lamivudine 100 mg group was −4.29 $\log_{10}$ copies/ml (Fig. 1; Table 2). Estimated mean differences (95% CI) in serum HBV DNA level (after adjustment for baseline level and HBeAg status) were −0.39 (−0.83 to 0.05) $\log_{10}$ copies/ml between the entecavir 0.1 mg and lamivudine 100 mg groups and −0.62 (−1.06 to −0.18) $\log_{10}$ copies/ml between the entecavir 0.5 mg and lamivudine 100 mg groups, indicating the noninferiority of the entecavir 0.1 and 0.5 mg groups to the lamivudine 100 mg group and the superiority of the entecavir 0.5 mg group to the lamivudine 100 mg group ($P = 0.007$) (Table 2). In contrast, the entecavir 0.01 mg group was significantly inferior to the lamivudine 100 mg group (estimated mean difference = 1.20 [0.69–1.71]; $P < 0.0001$) (Table 2).

The secondary efficacy end point of a reduction in serum HBV DNA level 2 $\log_{10}$ copies/ml or more or HBV DNA level less than 400 copies/ml by PCR assay was achieved by 88.6% of patients in the entecavir 0.01 mg group and by 100% of patients in the entecavir 0.1 and 0.5 mg groups at week 22. Ninety-seven percent of patients in the lamivudine 100 mg group achieved this end point at week 22. HBV DNA level less than 0.7 MEq/ml by bDNA assay was achieved by 65.7%, 94.1%, and 100% of patients in the 0.01, 0.1, and 0.5 mg entecavir groups, respectively, and by 93.9% of patients in the lamivudine 100 mg treatment group.

Serologic response

Among HBeAg-positive patients, there was no significant difference between seroconversion rates at week 22 for the entecavir 0.01, 0.1, and 0.5 mg treatment groups (10.0%, 13.3%, and 3.6%, respectively) versus the lamivudine 100 mg treatment group (3.3%; Table 2). All patients who lost HBeAg also experienced HBeAg seroconversion.

Biochemical response

At baseline, elevated serum ALT levels (>1.25 × ULN) were present in more than 90% of patients in all four treatment groups. At week 22, normal serum ALT levels (World Health Organization grade 0, <1.25 × ULN) were recorded in similar proportions of patients in the entecavir 0.01, 0.1, and 0.5 mg treatment groups (75.0%, 85.3%, and 80.0% of patients, respectively) and the lamivudine treatment group (78.1% of patients), with no significant intergroup difference (Table 2).

Response

Response (HBV DNA level <0.7 MEq/ml by bDNA assay, HBeAg loss, and serum ALT level <1.25 × ULN for HBeAg-positive patients and HBV DNA level <0.7 MEq/ml by bDNA assay and serum ALT <1.25 × ULN for HBeAg-negative patients) was achieved by 14.3%, 20.6%, and 15.6% of patients in the entecavir 0.01, 0.1, and 0.5 mg

Table 2 Differences in HBV DNA levels between entecavir dose groups by PCR at week 22 in evaluable subjects

	0.1 mg ETV–0.01 mg ETV ($n = 34$, $n = 35$)	0.5 mg ETV–0.01 mg ETV ($n = 32$, $n = 35$)	0.5 mg ETV–0.1 mg ETV ($n = 32$, $n = 34$)
Estimated difference[a] ($\log_{10}$ copies/ml)	−1.61	−1.95	−0.23
Standard error	0.24	0.24	0.19
95% Confidence interval[b]	−2.20, −1.02	−2.53, −1.37	−0.69, 0.23
P-value	<0.0001	<0.0001	0.227

[a] Estimated differences are regression-adjusted for baseline serum HBV DNA and HBeAg status

[b] 95% Confidence interval is adjusted by modified Bonferroni procedures

ETV entecavir

Table 3 Virology and biochemical responses at week 22 and comparison of entecavir treatment groups with lamivudine in evaluable subjects

Response	ETV 0.01 mg ($n = 35$)	ETV 0.1 mg ($n = 34$)	ETV 0.5 mg ($n = 32$)	LVD 100 mg ($n = 33$)
HBV DNA by PCR assay				
Reduction from baseline at week 22 (log_{10} copies/ml), mean ± S.E.	−3.11 ± 0.18	−4.77 ± 0.17	−5.16 ± 0.13	−4.29 ± 0.18
HBV DNA estimated difference[a] (vs. LVD) (log_{10} copies/ml)	1.20	−0.39	−0.62	–
Standard error	0.26	0.22	0.22	–
95% Confidence interval	0.69, 1.71	−0.83, 0.05	−1.06, -0.18	–
P-value	<0.0001[b]	0.081	0.007[c]	–
HBV DNA by Roche Amplicor™ PCR assay				
Change in log_{10} HBV DNA reduction >2 or HBV DNA <400 copies/ml at week 22, *n* (%)	31 (88.6)	34 (100)	32 (100)	32 (97.0)
P-value (vs. LVD)	0.206	NR[d]	NR[d]	–
HBV DNA by Quantiplex assay				
HBV DNA <0.7 MEq/ml (2.5 pg/ml) at week 22, *n* (%)	23 (65.7)	32 (94.1)	32 (100)	31 (93.9)
P-value (vs. LVD)	0.002	1.000	NR[d]	–
Normalization of ALT levels[e]				
At week 22, *n/n* with abnormal baseline (%)	24/32 (75.0)	29/34 (85.3)	24/30 (80.0)	25/32 (78.1)
P-value (vs. LVD)	0.842	0.439	0.880	–
Loss of HBeAg and seroconversion at week 48[f]				
HBeAg loss, n/n HBeAg positive at baseline (%)	3/30 (10.0)	4/30 (13.3)	1/28 (3.6)	1/30 (3.3)
HBeAg seroconversion	3/30 (10.0)	4/30 (13.3)	1/28 (3.6)	1/30 (3.3)
P-value (vs. LVD)	0.605	0.350	1.000	–
Response[g] at week 22, *n* (%)	5 (14.3)	7 (20.6)	5 (15.6)	3 (9.1)
P-value (vs. LVD)	0.735	0.190	0.480	–

[a] Estimated differences are regression-adjusted for baseline HBV DNA and HBeAg status

[b] Two-sided test indicates inferiority of the entecavir 0.01 mg dose

[c] Two-sided test indicates superiority of the entecavir dose

[d] Not reported because expected counts <5

[e] WHO grade 0, ALT <1.25 × upper limit of normal

[f] Seroconversion was defined as disappearance of HBe-antigen and appearance of HBe-antibody

[g] Response was defined as HBV DNA levels <0.7 MEq/ml, HBeAg negativity and ALT <1.25 × ULN for HBeAg-positive patients and HBV DNA levels <0.7 MEq/ml and ALT <1.25 × ULN for HBeAg-negative patients

ETV entecavir

LVD lamivudine

treatment groups, respectively, and by 9.1% of patients in the lamivudine treatment group at week 22, and there were no significant differences in the rates of response between the four treatment groups (Table 2).

Resistance analysis

During the treatment period, serum HBV DNA level increased by 1 log_{10} copies/ml or more from its nadir in one patient in the entecavir 0.01 mg group and one patient in the lamivudine 100 mg group. Nucleotide sequence analysis of the DNA polymerase coding region, using viral samples collected from these two patients at day 1 and at week 22, revealed no lamivudine-resistance substitutions (rt180 and rt204 amino acid residues) [17, 18] or entecavir-resistance substitutions (rt184, rt202, and rt250 amino acid residues) [19].

Safety

During the study, adverse events were experienced by similar proportions of patients in the entecavir 0.01, 0.1, and 0.5 mg groups and the lamivudine 100 mg treatment group (97.1%, 97.1%, 91.2%, and 100.0%, respectively). Most adverse events were of mild or moderate intensity (grade 1/2) and transient. The most frequently reported adverse events (affecting ≥ 10% of patients in any one treatment group) included nasopharyngitis, headache, and

Table 4 Summary of adverse events and laboratory abnormalities during the 24-week blinded treatment phase

	ETV 0.01 mg ($n = 35$)	ETV 0.1 mg ($n = 34$)	ETV 0.5 mg ($n = 34$)	LVD 100 mg ($n = 34$)
Any adverse events	34 (97)	33 (97)	31 (91)	34 (100)
Most frequent clinical adverse events,[a] *n* (%)				
Nasopharyngitis	9 (25.7)	10 (29.4)	11 (32.4)	10 (29.4)
Headache	6 (17.1)	7 (20.6)	2 (5.9)	7 (20.6)
Diarrhea	1 (2.9)	1 (2.9)	4 (11.8)	4 (11.8)
Grade 3/4 clinical adverse events, *n* (%)	0	0	1 (2.9)	1 (2.9)
Grade 3/4 laboratory adverse events, *n* (%)	2 (5.7)	4 (11.8)	2 (5.9)	4 (11.8)
Any serious adverse events, *n* (%)	0	1 (2.9)	2 (5.9)	1 (2.9)
Discontinuations due to adverse events,[b] *n* (%)	0	0	1 (2.9)	1 (2.9)
ALT flares,[c] *n* (%)	0	1 (2.9)	1 (2.9)	2 (5.9)
Death, *n* (%)	0	0	0	0

[a] Occurring in at least 10% of patients

[b] One patient treated with ETV 0.5 mg discontinued the study drug due to hepatic cirrhosis. One patient treated with lamivudine discontinued due to increased ALT

[c] ALT flare defined ALT >2 × baseline and 10 × ULN

ETV entecavir

LVD lamivudine

diarrhea (Table 4). Grade 3/4 clinical adverse events occurred in one patient in the entecavir 0.5 mg group (colon carcinoma) and one patient in the lamivudine group (anal ulcer); neither of these events was considered to be related to the study drug. Serious adverse events were limited to the above-mentioned case of colon carcinoma, serum ALT elevation (entecavir 0.1 mg group [$n = 1$], entecavir 0.5 mg group [$n = 1$]), and serum aspartate aminotransferase (AST)/ALT elevation (lamivudine 100 mg group [$n = 1$]), but these were not considered to be causally related to the study drug and did not necessitate treatment discontinuation. Transient ALT flares (serum ALT >2 × baseline level and >10 × ULN) occurred in four patients (entecavir 0.1 mg group [$n = 1$], entecavir 0.5 mg group [$n = 1$], and lamivudine 100 mg group [$n = 2$]) and were associated with HBV DNA level decreases of 2 $\log_{10}$ copies/ml or more. None of the ALT flares were associated with hepatic decompensation and serum ALT and AST levels recovered to less than 1.25 × baseline level on continuation of the study treatment.

Discussion

The global ETV-005 study reported that entecavir was superior to lamivudine at reducing viral load in nucleoside-naive patients with CHB infection [15]. We conducted the present study, using an identical design to the ETV-005 study, to determine whether the findings from this earlier study are applicable to Japanese patients. In keeping with the previous findings, our results indicate that entecavir produces a dose-related reduction in serum HBV DNA level ($0.01 < 0.1 \leq 0.5$ mg) in nucleoside-naive Japanese patients with CHB; the log dose–response curves for the reduction in serum HBV DNA level with entecavir in the two studies were similar, with estimated regression curve slopes of –1.24 (Japanese study) and –1.32 (global study). In addition, both studies demonstrated the noninferiority of the entecavir 0.1 mg group compared with the lamivudine 100 mg group and the superiority of the entecavir 0.5 mg group compared with the lamivudine 100 mg group. The demonstration of a dose–response relationship for entecavir and the superiority of the entecavir 0.5 mg dose over lamivudine confirm that the antiviral activity of entecavir in Japanese patients is similar to that observed in study ETV-005. In a previous study, Ono et al. [14] demonstrated that the in vitro potency of entecavir was up to 2,200 times greater than that of lamivudine. The results presented here substantiate these earlier in vitro data and confirm the greater potency of entecavir over lamivudine in patients with CHB.

Serum ALT normalization rates with entecavir 0.5 mg and lamivudine 100 mg (~80%) were higher in the present study than those reported in the ETV-005 study (entecavir 0.5 mg, 69.0%; lamivudine 100 mg, 59.1%) [15]. In keeping with previous findings [20, 21], the incidence of entecavir-associated serum ALT flares in Japanese patients was low. The serum ALT flares occurred against a background of 2 $\log_{10}$ copies/ml or more reductions in serum

HBV DNA level, and serum ALT levels subsequently normalized without discontinuation of entecavir. Therefore, the serum ALT flare noted here may indicate recovery of the host's immune response arising from the reduction in HBV viral titer [22, 23]. ALT flares have been reported after the discontinuation of entecavir therapy [15, 16], thus necessitating long-term follow-up to identify possible posttreatment viral rebound.

In conclusion, the results of this dose-ranging study demonstrate a clear dose–response relationship for entecavir in terms of mean HBV DNA level reduction at week 22. Entecavir 0.5 mg was significantly more effective than lamivudine 100 mg in reducing HBV DNA levels in nucleoside-naive Japanese adult patients with CHB. At this dose level, entecavir treatment resulted in serum HBV DNA levels of less than 400 copies/ml in 100% of patients and normalization of serum ALT levels in 80% of patients after 22 weeks. Moreover, entecavir 0.5 mg once daily was well tolerated and showed a comparable safety profile to lamivudine.

References

1. Maddrey WC. Hepatitis B: an important public health issue. J Med Virol 2000;61:362–366. doi:10.1002/1096-9071(200007)61:3<362::AID-JMV14>3.0.CO;2-I
2. Kao JH, Chen DS. The natural history of hepatitis B virus infection. In Lai CL, Locarnini S, editors. Hepatitis B Virus. London: International Medical Press; 2002. 161–172
3. Lok AS, McMahon BJ. American Association for the Study of Liver Diseases (AASLD) practice guidelines. Chronic Hepatitis B. Hepatology 2007;45:507–539. doi:10.1002/hep.21513
4. Rivkin A. A review of entecavir in the treatment of chronic hepatitis B infection. Curr Med Res Opin 2005;21:1845–1856. doi:10.1185/030079905X65268
5. Wong DKH, Cheung AM, O'Rourke K, Naylor CD, Detsky AS, Heathcote J. Effect of alpha-interferon treatment in patients with hepatitis B e antigen-positive chronic hepatitis B. A meta-analysis. Ann Intern Med 1993;119:312–323
6. Allen MI, Deslauriers M, Andrews CW, Tipples GA, Walters KA, Tyrrell DL, et al. Identification and characterization of mutations in hepatitis B virus resistant to lamivudine. Lamivudine Clinical Investigation Group. Hepatology 1998;27:1670–1677. doi:10.1002/hep.510270628
7. Chang TT, Lai CL, Chien RN, Guan R, Lim SG, Lee CM, et al. Four years of lamivudine treatment in Chinese patients with chronic hepatitis B. J Gastroenterol Hepatol 2004;19(11):1276–1282. doi:10.1111/j.1440-1746.2004.03428.x
8. Liaw YF, Sung JJ, Chow WC, Farrell G, Lee CZ, Yuen H, et al. Lamivudine for patients with chronic hepatitis B and advanced liver disease. N Engl J Med 2004;351(15):1521–1531. doi:10.1056/NEJMoa033364
9. Omata M. Treatment of chronic hepatitis B infection. N Engl J Med 1998;339:114. doi:10.1056/NEJM199807093390209
10. Liaw YF, Leung N, Kao JH, Piratvisuth T, Gane E, Han KH, et al. Asian-Pacific consensus statement on the management of chronic hepatitis B: a 2008 update. Hepatol Int 2008;2:263–283. doi:10.1007/s12072-008-9080-3
11. Genovesi EV, Lamb L, Medina I, Taylor D, Seifer M, Innaimo S, et al. Efficacy of the carbocyclic 2′-deoxyguanosine nucleoside BMS-200475 in the woodchuck model of hepatitis B virus infection. Antimicrob Agents Chemother 1998;42:3209–3217
12. Marion PL, Salazar FH, Winters MA, Colonno RJ. Potent efficacy of entecavir (BMS-200475) in a duck model of hepatitis B virus replication. Antimicrob Agents Chemother 2002;46:82–88. doi:10.1128/AAC.46.1.82-88.2002
13. Colonno RJ, Rose R, Baldick CJ, Levine S, Pokornowski K, Yu CF, et al. Entecavir resistance is rare in nucleoside naïve patients with hepatitis B. Hepatology 2006;44:1656–1665. doi:10.1002/hep.21422
14. Ono SK, Kato N, Shiratori Y, Kato J, Goto T, Schinazi RF, et al. The polymerase L528M mutation cooperates with nucleotide binding-site mutations, increasing hepatitis B virus replication and drug resistance. J Clin Invest 2001;107:449–455. doi:10.1172/JCI11100
15. Lai CL, Rosmawati M, Lao J, Van Vlierberghe H, Anderson FH, Thomas N, et al. Entecavir is superior to lamivudine in reducing hepatitis B virus DNA in patients with chronic hepatitis B infection. Gastroenterology 2002;123:1831–1838. doi:10.1053/gast.2002.37058
16. Chang TT, Gish RG, Hadziyannis SJ, Cianciara J, Rizzetto M, Schiff ER, et al. A dose-ranging study of the efficacy and tolerability of entecavir in lamivudine-refractory chronic hepatitis B patients. Gastroenterology 2005;129:1198–1209. doi:10.1053/j.gastro.2005.06.055
17. Ling R, Mutimer D, Ahmed M, Boxall EH, Elias E, Dusheiko GM, et al. Selection of mutations in the hepatitis B virus polymerase during therapy of transplant recipients with lamivudine. Hepatology 1996;24:711–713. doi:10.1002/hep.510240339
18. Tipples GA, Ma MM, Fischer KP, Bain VG, Kneteman NM, Tyrrell DLJ. Mutation in HBV RNA-dependent DNA polymerase confers resistance to lamivudine in vivo. Hepatology 1996;24:714–717
19. Tenney DJ, Levine SM, Rose RE, Walsh AW, Weinheimer SP, Discotto L, et al. Clinical emergence of entecavir-resistant hepatitis B virus requires additional substitutions in virus already resistant to lamivudine. Antimicrob Agents Chemother 2004;48:3498–3507. doi:10.1128/AAC.48.9.3498-3507.2004
20. Chang TT, Gish R, de Man R, Gadano A, Sollano J, Chao YC, et al. A comparison of entecavir and lamivudine for HBeAg-positive chronic hepatitis B. N Engl J Med 2006;354:1074–1076. doi:10.1056/NEJMoa051285
21. Sherman M, Yurdaydin C, Sollano J, Silva M, Liaw Y-F, Cianciara J, et al. Entecavir is superior to continued lamivudine for the treatment of lamivudine-refractory. HBeAg-positive chronic hepatitis B. Gastroenterology 2006;130:2039–2049
22. Boni C, Bertoletti A, Penna A, Cavalli A, Pilli M, Urbani S, et al. Lamivudine treatment can restore T cell responsiveness in chronic hepatitis B. J Clin Invest 1998;102:968–975. doi:10.1172/JCI3731
23. Nair S, Perrillo RP. Serum alanine aminotransferase flares during interferon treatment of chronic hepatitis B: is sustained clearance of HBV DNA dependent on levels of pretreatment viremia? Hepatology 2001;34:1021–1026. doi:10.1053/jhep.2001.28459

BMS9RJ3389

RESEARCH ARTICLES

ERK5 is a Target for Gene Amplification at 17p11 and Promotes Cell Growth in Hepatocellular Carcinoma by Regulating Mitotic Entry

Keika Zen,[1] Kohichiroh Yasui,[1]* Tomoaki Nakajima,[1] Yoh Zen,[2] Kan Zen,[3] Yasuyuki Gen,[1] Hironori Mitsuyoshi,[1] Masahito Minami,[1] Shoji Mitsufuji,[1] Shinji Tanaka,[4] Yoshito Itoh,[1] Yasuni Nakanuma,[2] Masafumi Taniwaki,[5] Shigeki Arii,[4] Takeshi Okanoue,[1] and Toshikazu Yoshikawa[1]

[1]Molecular Gastroenterology and Hepatology, Graduate School of Medical Science, Kyoto Prefectural University of Medicine, Kyoto, Japan
[2]Department of Human Pathology, Kanazawa University Graduate School of Medicine, Kanazawa, Japan
[3]Division of Cardiovascular Medicine, Omihachiman Community Medical Center, Omihachiman, Japan
[4]Department of Hepato-Biliary-Pancreatic Surgery, Tokyo Medical and Dental University, Tokyo, Japan
[5]Molecular Hematology and Oncology, Graduate School of Medical Science, Kyoto Prefectural University of Medicine, Kyoto, Japan

Using high-density oligonucleotide microarrays, we investigated DNA copy-number aberrations in cell lines derived from hepatocellular carcinomas (HCCs) and detected a novel amplification at 17p11. To identify the target of amplification at 17p11, we defined the extent of the amplicon and examined HCC cell lines for expression of all seven genes in the 750-kb commonly amplified region. Mitogen-activated protein kinase (MAPK) 7, which encodes extracellular-regulated protein kinase (ERK) 5, was overexpressed in cell lines in which the gene was amplified. An increase in *MAPK7* copy number was detected in 35 of 66 primary HCC tumors. Downregulation of *MAPK7* by small interfering RNA suppressed the growth of SNU449 cells, the HCC cell line with the greatest amplification and overexpression of *MAPK7*. ERK5, phosphorylated during the G2/M phases of the cell cycle, regulated entry into mitosis in SNU449 cells. In conclusion, our results suggest that *MAPK7* is likely the target of 17p11 amplification and that the ERK5 protein product of *MAPK7* promotes the growth of HCC cells by regulating mitotic entry.

INTRODUCTION

Hepatocellular carcinoma (HCC) is the fifth most common malignancy in the world and is estimated to cause approximately half a million deaths annually (El-Serag, 2002). Several risk factors for HCC have been reported, including infection with hepatitis B and C viruses, dietary intake of afratoxin, alcohol consumption, and diabetes.

The mitogen-activated protein kinase (MAPK) cascades transmit extracellular signals from cell surface receptors to specific intracellular targets and regulate a wide variety of cellular functions, including cell proliferation, differentiation, and the stress response (Nishimoto and Nishida, 2006). Extracellular stimuli induce sequential activation of MAPK kinase kinase, MAPK kinase, and MAPK. At least four MAPK subfamilies have been identified: extracellular-regulated protein kinase (ERK) 1 and 2, c-Jun-N-terminal kinases, p38, and ERK5 (also know as BMK1). ERK5, which was recently characterized, can be activated by a wide range of growth factors and cellular stresses, including serum, epithelial growth factor, oxidative stress, and hyperosmotic shock (Hayashi and Lee, 2004; Nishimoto and Nishida, 2006; Wang and Tournier, 2006). When stimulated, MAP/ERK kinase kinase 2 and 3 activate MAP/ERK kinase (MEK) 5, a specific kinase for ERK5. Subsequently, MEK5 phosphorylates ERK5, and the activated ERK5 promotes cell proliferation, differentiation, and survival (Hayashi and Lee, 2004; Garaude et al., 2006; Nishimoto and Nishida, 2006; Wang and Tournier, 2006). Some investigators have described the possible involvement of ERK5 in cancers (Esparis-Ogando et al., 2002; Weldon et al., 2002; Mulloy et al., 2003; Carvajal-Vergara et al., 2005; Linnerth et al., 2005).

Additional Supporting Information may be found in the online version of this article.

Supported by: Grants-in-Aid for Scientific Research from the Japan Society for the Program of Science, Grant number: 18390223.

*Correspondence to: Kohichiroh Yasui, Molecular Gastroenterology and Hepatology, Graduate School of Medical Science, Kyoto Prefectural University of Medicine, 465 Kajii-cho, Kamigyo-ku, Kyoto, 602-8566, Japan. E-mail: yasuik@koto.kpu-m.ac.jp

Received 24 May 2008; Accepted 11 September 2008

DOI 10.1002/gcc.20624

Published online 30 October 2008 in Wiley InterScience (www.interscience.wiley.com).

Accumulating evidence suggests that multiple sequential genetic alterations in a cell lineage at the nucleotide and chromosome levels underlie the carcinogenesis of solid tumors. Amplification of chromosomal DNA is one mechanism of activating genes whose overexpression contributes to the development and progression of cancer. Regions of chromosomal amplification in cancer cells frequently harbor oncogenes, such as *MYC* (Little et al., 1983) and *ERBB2* (Di Fiore et al., 1987). Using comparative genomic hybridization (CGH), we have detected novel regions of amplification in a variety of cancer types, including HCC, and we have identified a number of candidate oncogenes from amplicons (Yasui et al., 2001; Yasui et al., 2002; Yokoi et al., 2002; Okamoto et al., 2003; Yokoi et al., 2003). CGH was initially used for genome-wide detection of copy number changes occurring in cancers (Kallioniemi et al., 1992). However, its resolution is limited (5–10 Mb) because it detects segmental copy number changes on metaphase chromosomes.

The recent introduction of high-density oligonucleotide microarrays designed for typing of single nucleotide polymorphisms (SNPs) facilitates high-resolution mapping of chromosomal amplifications, deletions, and loss of heterozygosity (Mei et al., 2000; Bignell et al., 2004; Matsuzaki et al., 2004a,b; Wong et al., 2004; Zhao et al., 2004). The Affymetrix GeneChip Mapping 100K array set contains 116,204 SNP loci with a mean intermarker distance of 23.6 kb, and it enables detailed and genome-wide identification of DNA copy number changes (Matsuzaki et al., 2004a,b; Garraway et al., 2005; Zhao et al., 2005). The newer GeneChip Mapping 500K array set is composed of two arrays, each capable of genotyping an average 250,000 SNPs.

In the work reported here, we investigated DNA copy number aberrations in HCC cell lines using Affymetrix high-density SNP arrays. We identified a novel amplification at 17p11 in HCC cell lines. This region may harbor one or more genes that, when amplified, contribute to carcinogenesis. Within the amplicon, *MAPK7*, which encodes ERK5, emerged as a probable target gene that acts as a driving force for amplification of the region and promotes the growth of HCC cells by regulating entry into mitosis.

MATERIALS AND METHODS

Cell Lines and Tumor Samples

A total of 21 liver cancer cell lines [HCC-derived HLE, HLF (Dor et al., 1975), PLC/PRF/5 (Alexander et al., 1976), Li7 (Hirohashi et al., 1979), Huh7 (Nakabayashi et al., 1982), Hep3B (Aden et al., 1979), SNU354, SNU368, SNU387, SNU398, SNU423, SNU449, SNU475 (Park et al., 1995), JHH-1, JHH-2, JHH-4, JHH-5, JHH-6, JHH-7 (Fujise et al., 1990), Huh-1 (Huh et al., 1981), and the hepatoblastoma line HepG2 (Knowles et al., 1980)] were examined in this study. All cell lines were maintained in Dulbecco's modified Eagle's medium supplemented with 10% fetal bovine serum. We obtained 66 primary HCC tumors for analysis of the DNA copy number of *MAPK7* from patients undergoing surgery at the hospitals of Tokyo Medical and Dental University and Kyoto University, Japan. Genomic DNA was isolated from each cell line and from 66 primary tumors using the Puregene DNA isolation kit (Gentra, Minneapolis, MN). For immunohistochemical studies of ERK5, 43 additional HCC samples were obtained from the Hospital of Kyoto Prefectural University of Medicine, Japan. Before initiation of the present study, informed consent was obtained in the formal style approved by all relevant ethical committees.

SNP Assay

The GeneChip Mapping 100K array set and GeneChip Mapping 250K Sty array (Affymetrix, Santa Clara, CA) were used in this study. Analyses were performed according to the manufacturer's instructions. In brief, 250 ng of genomic DNA was digested with a restriction enzyme (*Xba*I or *Hind*III for the 100K array set and *Sty*I for the 250K Sty array), ligated to an adaptor, and amplified by PCR (Kennedy et al., 2003; Matsuzaki et al., 2004a,b; Zhao et al., 2004). Amplified products were fragmented, labeled by biotinylation, and hybridized to the microarrays. Hybridization was detected by incubation with a streptavidin-phycoerythrin conjugate, followed by scanning of the array, and analysis was performed as described previously (Kennedy et al., 2003; Di et al., 2005). Copy number changes were calculated using the Copy Number Analyzer for Affymetrix GeneChip Mapping Arrays (http://www.genome.umin.jp) (Nannya et al., 2005).

Fluorescence In Situ Hybridization

We performed FISH using the bacterial artificial chromosome (BAC) RP11-73E4 as a probe (Invitrogen, Carlsbad, CA) as described previously (Yasui et al., 2002). The BAC was selected

on the basis of its location according to the database provided by the UCSC (http://genome.ucsc.edu/). Briefly, the probe was labeled by nick translation with biotin-16-dUTP (Roche Diagnostics, Penzberg, Germany) and hybridized to metaphase chromosomes. Hybridization signals for biotin-labeled probes were detected with avidin-fluorescein (Roche Diagnostics).

Real-Time Quantitative PCR

We quantified genomic DNA and mRNA using a real-time fluorescence detection method. Total RNA was obtained using Trizol (Invitrogen). Residual genomic DNA was removed by incubating the RNA samples with RNase-free DNase I (Takara Bio, Shiga, Japan) prior to reverse transcription (RT)-PCR. Single-stranded complementary DNA was generated using superscript III reverse transcriptase (Invitrogen) according to the manufacturer's directions. Real-time quantitative PCR experiments were performed with the LightCycler system using FastStart DNA Master Plus SYBR Green I (Roche Diagnostics) according to the manufacturer's protocol. The primers were as follows: *MAPK7* DNA (forward, 5′-TGCTGACTGGCTCGAAG-3′; reverse, 5′-GGGTCTGAGATGAACCTGC-3′); *MAPK7* mRNA (forward, 5′-TTTGCCTTACTTCCCACCTG-3′; reverse, 5′-CCCATGTCGAAAGACTGGTT-3′); *GRAP* mRNA (forward, 5′-TCGAAGGACAGACTGCACAC-3′; reverse, 5′-AGAAGAGGAGTGTGCCTCCA-3′); *EPN2* mRNA (forward, 5′-TCACCTCACCCACCACTGTA-3′; reverse, 5′-GTGGTCAGCTGCCCTTAGAG-3′); *EPPB9* mRNA (forward, 5′-CTTTGTGTACGGCCAGGACT-3′; reverse, 5′-CGTAGGGGTTGGTGCTTTTA-3′); *MFAP4* mRNA (forward, 5′-GGTGACTCCCTGTCCTACCA-3′; reverse, 5′-TCATCTCAGTGCGTTTGAGG-3′); *ZNF179* mRNA (forward, 5′-ACTGGGCAGAACCAGAGAGA-3′; reverse, 5′-AGGATGCACAGACAGGCTCT-3′); *FLJ10847* mRNA (forward, 5′-AACTCTTGGGCTTCAAGCAA-3′; reverse, 5′-AGGAGGTTGAGGCTGCAGTA -3′). These primers were designed using Primer3 (http://frodo.wi.mit.edu/cgi-bin/primer3/primer3_www.cgi) on the basis of sequence data obtained from the NCBI database (http://www.ncbi.nlm.nih.gov/). *GAPDH* (Minamiya et al., 2004) and long interspersed nuclear element (LINE)-1 (Zhao et al., 2004) were used as endogenous controls for mRNA and genomic DNA levels, respectively.

Immunoblotting

Immunoblots were prepared according to previously reported methods (Yasui et al., 2001). Cell lysates (20 μg protein per sample) were separated by sodium dodecyl sulfate-polyacrylamide gel electrophoresis on 10% acrylamide gels. We obtained the following antibodies from Sigma-Aldrich (Tokyo, Japan): anti-ERK5 polyclonal antibody, anti-phospho-ERK5 (pThr218/pThr220) polyclonal antibody, and anti-β-actin monoclonal antibody. For immunoblotting, we used anti-ERK5, anti-phospho-ERK5, and anti-β-actin at dilutions of 1:500, 1:1000, and 1:5000, respectively. For secondary immunodetection, we used anti-rabbit or anti-mouse Ig (Amersham, Tokyo, Japan) diluted 1:5000. Protein binding was detected using the ECL system (Amersham).

Immunoprecipitation

Cells were lysed with RIPA buffer (10 mM Tris-HCl, pH 7.4, 150 mM NaCl, 1% Triton X-100, 0.1% sodium dodecyl sulfate, 1% sodium deoxycholate, 1 mM phenylmethylsulfonyl fluoride), and incubated on ice for 30 min. The lysate was centrifuged at 14,000 × *g* at 4°C for 15 min. The supernatant was incubated with normal rabbit IgG and protein A-agarose beads (Santa Cruz Biotechnology, Santa Cruz, CA) to decrease nonspecific protein binding. After centrifugation, the supernatant was incubated with anti-ERK5 polyclonal antibody or normal rabbit IgG (control) overnight at 4°C. Protein A-agarose beads were added to the reaction and the mixture was incubated for an additional 1 hr. The precipitates were recovered by a brief centrifugation, followed by four washes with RIPA buffer. Samples were then boiled in electrophoresis sample buffer and separated by electrophoresis as described above (see "Immunoblotting" section).

Immunohistochemical Analysis

Forty-three primary HCCs, consisting of paired tumor and surrounding nontumor tissues, and two HCC cell lines (SNU449 and Li7) were analyzed by anti-ERK5 immunostaining. Immunohistochemical staining was performed on formalin-fixed and paraffin-embedded sections using an anti-ERK5 polyclonal antibody (Sigma-Aldrich) at a 1:200 dilution. An automated tissue immunostainer (Ventana Medical Systems, Tucson, AZ) was used according to the manufacturer's instructions. The staining was developed with 3,3′-

diaminobenzidine tetrahydrochloride, followed by counterstaining with hematoxylin.

Growth Assays and RNA Interference Studies

For cell growth assays viable cells were stained with 0.2% trypan blue and counted with a hemocytometer 24, 48, and 72 hr after transfection. For RNA interference (RNAi) studies, Stealth small interfering RNA (siRNA) duplex oligoribonucleotides targeting *MAPK7* (5′-CCAUGGCAUGAAC CCUGCCGAUAUU-3′) and Stealth RNAi negative control duplexes were synthesized by Invitrogen. The siRNAs were delivered into SNU449 cells using Lipofectamine 2000 (Invitrogen) according to the manufacturer's instructions. To determine mRNA levels, cells were harvested 48 hr after transfection and subjected to quantitative RT-PCR as described above.

Cell Cycle Synchronization

SNU449 cells were synchronized at G1/S, early S, or M phases. For G1/S or early S-phase synchronization, cells were incubated in medium containing 2.5 mM thymidine (Sigma Chemical Co., St. Louis, MO) for 24 hr, followed by 12 hr in medium without thymidine, and finally another 12 hr in medium containing 2.5 mM thymidine (double-thymidine block; for G1/S-phase) or 1 μg/ml aphidicolin (early S-phase block). For M phase synchronization, cells were incubated in medium containing 2.5 mM thymidine for 24 hr, followed by 4 hr in medium without thymidine, and finally another 12 hr in medium containing 0.5 μg/ml nocodazole.

Cell Cycle Analysis

SNU449 cells were synchronized at the G1/S-phase boundary by a double-thymidine block as described above. Synchronized cells were released into fresh medium without thymidine and harvested at the indicated time points. These cells were then stained with propidium iodide and analyzed using a FACSCaliber scanner and Cell Quest software (Becton Dickinson Pharmingen, San Diego, CA).

Mitotic Index

Cells were grown in 24-well plates and transfected with Stealth RNAi targeting *MAPK7* or Stealth RNAi negative control duplexes as described above (see "Growth Assays and RNA Interference Studies" section). After 24 hr, cells were synchronized at the G1/S-phase boundary by a double-thymidine block. Synchronized cells were collected, reseeded on glass slides, and incubated for an additional 9 hr in fresh medium without thymidine. Next, the cells were stained with an anti-phospho-histone H3 antibody that specifically detects mitotic cells. Briefly, cells were fixed with 3.7% formaldehyde, permeabilized with 0.25% Triton X-100, and incubated with PBS containing 1% bovine serum albumin. The cells were then treated with a mixture of 4 μg/ml anti-phospho-histone H3 (Ser10)-biotin conjugated antibody (Upstate Biotechnology, Lake Placid, NY) and a 1:100 dilution of streptavidin-fluorescein (Roche Diagnostics) for 1 hr at room temperature, followed by counterstaining with propidium iodide. Positive staining for phospho-histone H3 was quantified by counting stained cells under a fluorescence microscope and dividing by the number of total cells. The mitotic index was scored as the percentage of mitotic cells in a population. On average, 200 cells were scored in three separate areas.

Statistical Analysis

All statistical analyses were performed using SPSS 15.0 software (SPSS Inc., Chicago, IL). Chi-square tests or analysis of variance (ANOVA) were used. P values < 0.05 were considered significant.

RESULTS

Detection of the 17p11 Amplicon in HCC Cell Lines by SNP Array Analysis

We screened for DNA copy number aberrations in 20 HCC cell lines by SNP array analysis. Two of the 20 cell lines, SNU449 and JHH-7, exhibited amplifications at chromosomal band 17p11 (Fig. 1A). In particular, the SNU449 cell line showed a high level of amplification in a narrow region on 17p11. We were able to define the smallest commonly affected region in the 17p11 amplicon as that lying between the positions recognized by the Affymetrix SNP_A-1662618 and SNP_A-1720748 probes (Fig. 1B). This region includes seven known or predicted protein-coding genes, *GRAP*, *EPN2*, *EPPB9*, *MAPK7*, *MFAP4*, *ZNF179*, and *FLJ10847*. The size of the amplicon was estimated to be approximately 750 kb.

To confirm amplification at 17p11 in SNU449 cells, we performed FISH analysis. The probe for

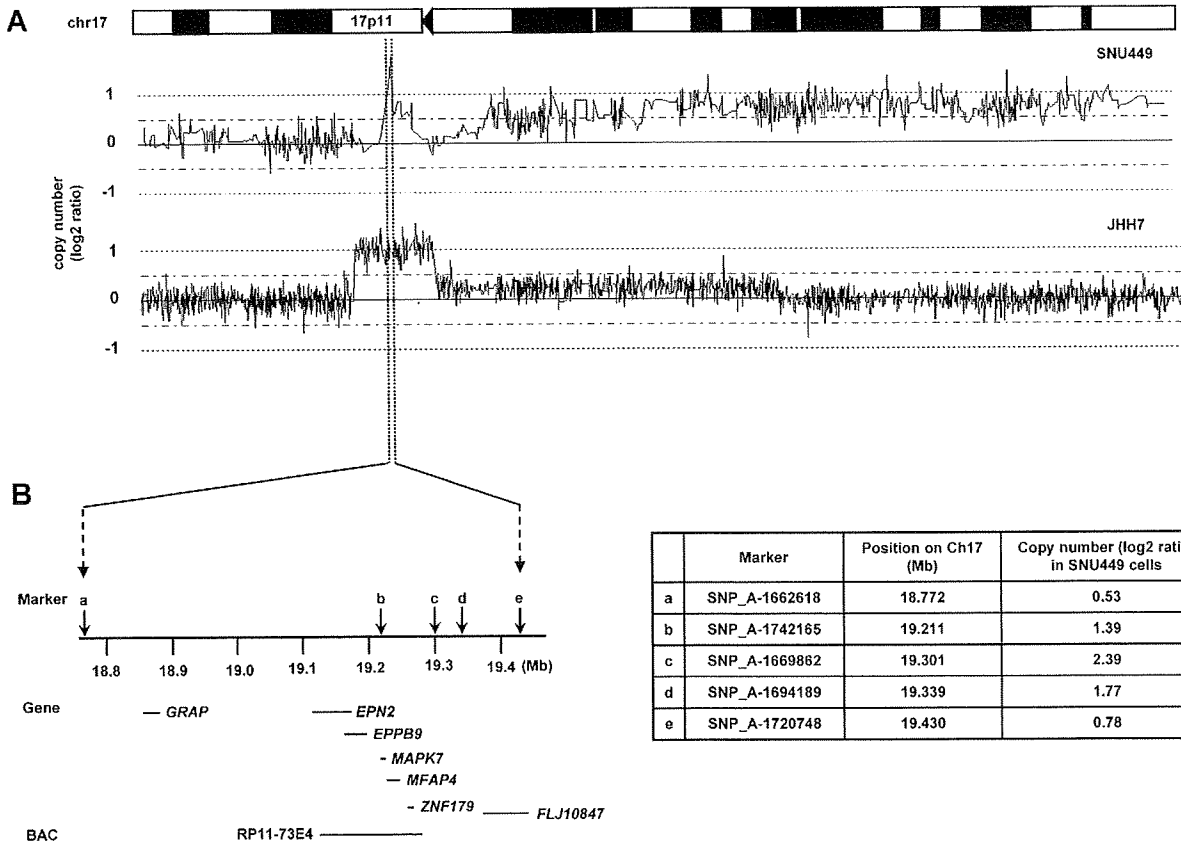

	Marker	Position on Ch17 (Mb)	Copy number (log2 ratio) in SNU449 cells
a	SNP_A-1662618	18.772	0.53
b	SNP_A-1742165	19.211	1.39
c	SNP_A-1669862	19.301	2.39
d	SNP_A-1694189	19.339	1.77
e	SNP_A-1720748	19.430	0.78

Figure 1. Map of the amplicon at 17p11 in two HCC cell lines. A: Copy number profiles for chromosome 17 in SNU449 and JHH-7 cells. Copy number values were determined by SNP 100K and 250K array analyses for SNU449 and JHH-7 cells, respectively. B: The smallest common region of amplification in SNU449 and JHH-7 cells (left). The position of the Affymetrix SNP markers, the seven genes within the amplicon (*GRAP*, *EPN2*, *EPPB9*, *MAPK7*, *MFAP4*, *ZNF179*, and *FLJ10847*) and the BAC RP11-73E4 (used as a probe for FISH) are numbered according to the UCSC genome database (http://genome.ucsc.edu/). Detailed copy-number information at positions identified by individual SNP markers over the amplified region in SNU449 cells is shown at right.

these experiments was BAC RP11-73E4, which contains *EPN2*, *EPPB9*, *MAPK7*, *MFAP4*, and *ZNF179* (Fig. 1B). This probe showed an amplified FISH signal on metaphase chromosomes from SNU449 cells (Fig. 2A). To further characterize the relationship between the genes in this chromosomal region and amplifications observed in cancer cells, we analyzed the gene dosage of the *MAPK7* locus by real-time quantitative PCR of DNA from 21 different liver cancer cell lines (20 HCC cell lines and the hepatoblastoma line HepG2). Amplification of *MAPK7* was observed in SNU449 and JHH-7 cells (Fig. 2B). Taken together, the data provide strong evidence that the 17p11 region is amplified in SNU449 and JHH-7 cells.

Analysis of Positional Candidate Genes in HCC Cell Lines

The 17p11 region may harbor one or more genes (henceforth referred to as "target genes") that, when activated by amplification, play a role in carcinogenesis. A common criterion for designating a gene as a putative target is that amplification leads to its overexpression (Collins et al., 1998). Thus, using real-time quantitative PCR, we determined the mRNA levels of all seven genes in the 17p11 amplicon in our panel of 21 liver cancer cell lines. As shown in Fig. 2C, the *EPN2*, *EPPB9*, and *MAPK7* genes were overexpressed in both SNU449 and JHH-7 cells. In several other lines, one or more of these three genes was overexpressed, despite the fact that regional amplification was not observed. These findings suggest that *EPN2*, *EPPB9*, and *MAPK7* are candidate target genes for 17p11 amplification.

Of these three genes, we chose to focus further analysis on *MAPK7*, which encodes ERK5, because ERK5-related proteins have been previously implicated in carcinogenesis (Hayashi and Lee, 2004; Wang and Tournier, 2006), whereas there is little or no evidence linking *EPN2* or

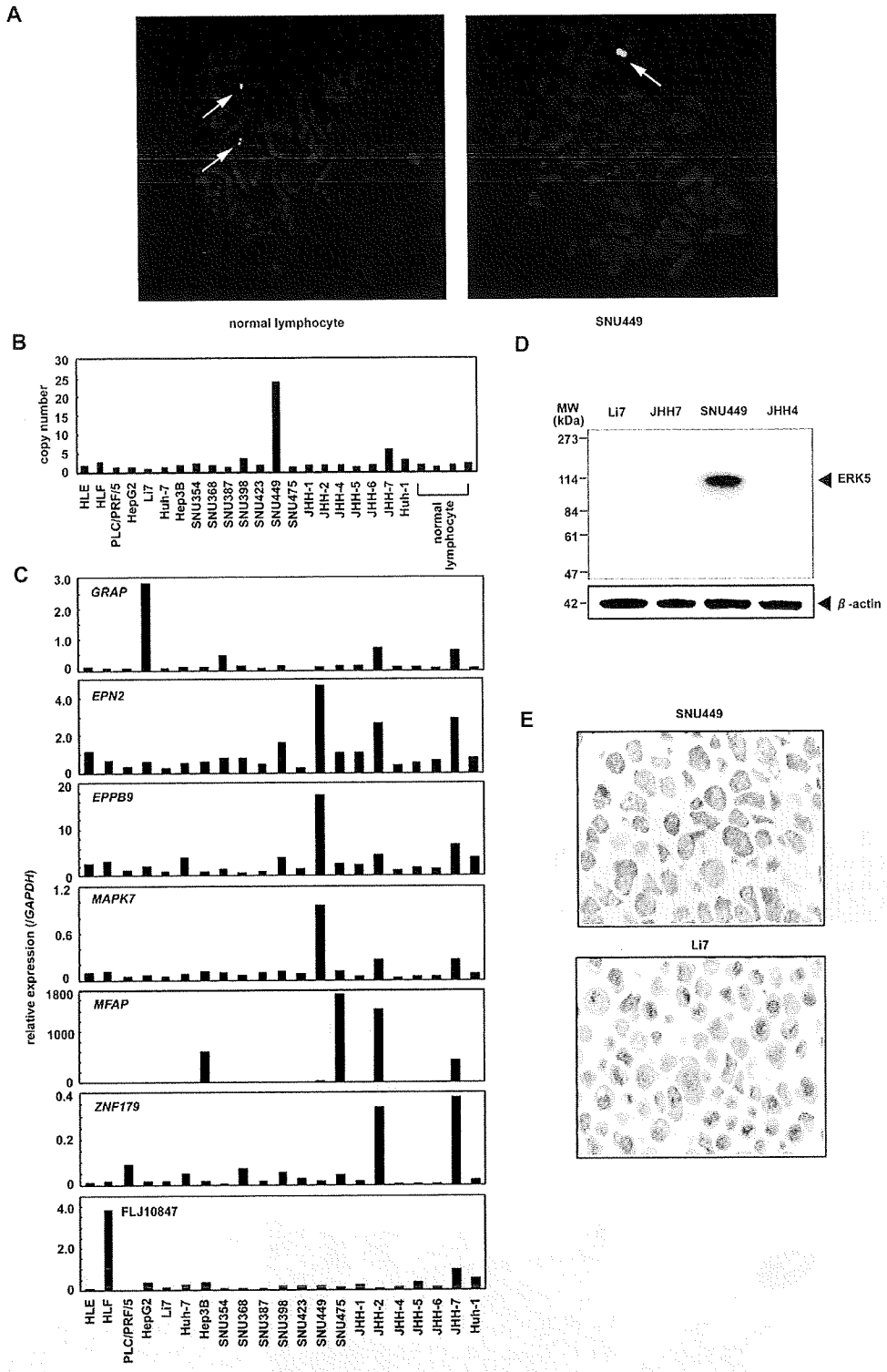

Figure 2. Amplification and overexpression of *MAPK7* in HCC cell lines. (A) Representative images from FISH analysis using a BAC RP11-73E4 probe on metaphase chromosomes from normal lymphocytes and SNU449 cells. While the probe shows a normal signal pattern (2 copies/cell) in normal lymphocytes (arrows, left), it shows an amplified signal in SNU449 cells (arrow, right). (B) Copy number of *MAPK7* in 21 liver cancer cell lines (20 HCC cells and one hepatoblastoma line, HepG2) and four peripheral blood lymphocytes (normal cell controls) as measured by real-time quantitative PCR with reference to a LINE-1 control. Values were normalized such that the average copy number of *MAPK7* in genomic DNA derived from normal lymphocytes is 2. (C) Relative expression levels of the seven genes within the 17p11 amplicon in a panel of 21 liver cancer cell lines as determined by real-time quantitative RT-PCR. The results are presented as the ratio between the expression level of each gene and a reference gene (*GAPDH*) to correct for variation in the amount of RNA. (D) Immunoblot analysis to detect protein levels of ERK5 and β-actin, an internal control, in four HCC cell lines with different *MAPK7* DNA copy numbers (B) and mRNA levels (C). (E) Immunostaining of ERK5 in SNU449 and Li7 cells.

EPPB9 to tumorigenesis. Immunoblot analysis revealed that ERK5 expression is upregulated in SNU449 cells. Indeed, among the HCC cell lines that were tested, SNU449 showed the highest level of both 17p11 amplification and *MAPK7* overexpression (Fig. 2D). Moreover, immunostaining confirmed that the level of ERK5 was elevated in SNU449 cells. ERK5 was strongly expressed in the cytoplasm of SNU449 cells (Fig. 2E). In contrast, ERK5 was weakly expressed in only a few Li7 cells, a HCC cell line that shows neither amplification nor overexpression of *MAPK7* (Fig. 2E).

Copy Number Gain of *MAPK7* in Primary HCC Tumors

To determine whether *MAPK7* is amplified in primary tumors, we examined 66 primary HCCs for copy number gains using real-time quantitative PCR. Copy number changes were counted as gains if the results of the analysis for a given tumor cell type exceeded the mean plus twice the standard deviation (SD) of the levels of *MAPK7* observed in genomic DNA derived from four peripheral blood lymphocyte samples (i.e., normal cells). A copy number gain for *MAPK7* was observed in 35 of the 66 tumors (53%; Fig. 3).

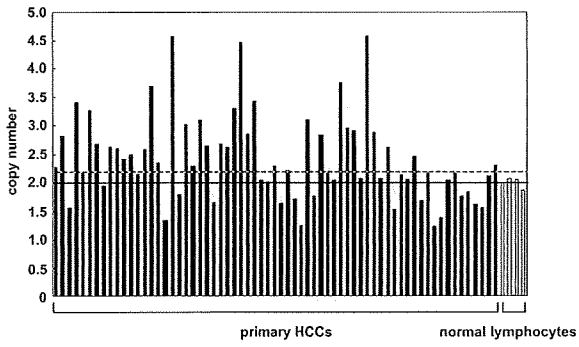

Figure 3. Copy number gain of *MAPK7* in primary HCC tumors. Copy numbers of *MAPK7* in 66 primary HCC tumors and four normal peripheral blood lymphocytes were determined by real-time quantitative PCR with reference to a LINE-1 control. Values were normalized such that the average copy number of *MAPK7* in genomic DNA derived from the normal lymphocytes equals 2 (solid horizontal line). The mean + 2 × SD of normal lymphocytes was used as the cutoff value for copy number gain (dotted line).

Expression of ERK5 in Primary HCCs

We next examined the level of ERK5 in 43 additional primary HCCs, including paired tumor and surrounding nontumor tissues. Immunohistochemical studies revealed that, in nontumor tissues (normal liver, chronic hepatitis, or liver cirrhosis), ERK5 is strongly expressed in bile ducts, bile ductules, and a few small hepatocytes (Fig. 4A). In these cells, ERK5 was present in the cytoplasm. Hepatocytes also contained ERK5, although at a lower level than in bile ducts (Fig. 4A). The staining pattern for ERK5 was almost identical for normal liver, chronic hepatitis, and liver cirrhosis.

This granular cytoplasmic staining for ERK5 was also observed in HCC cancer cells (Fig. 4B). HCC cells containing ERK5 were uniformly distributed in the tumor tissues. The level of ERK5 was elevated in 11 of the 43 tumors compared with the paired nontumor tissues (Figs. 4B and 4C; Supp. Info. Table 1). To clarify the relationship between the level of ERK5 and various clinicopathological parameters, we examined available data from the 43 patients, whose tumors were divided into elevated (T>NT) and not elevated (T≤NT) groups. There was no significant correlation between the level of ERK5 and any parameter examined, including age and gender of the patients; size, stage, and degree of differentiation of the tumor; HBV or HCV infection; and

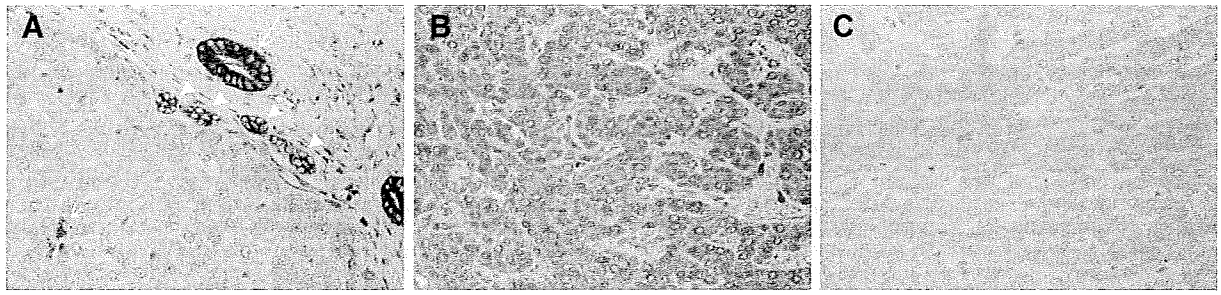

Figure 4. Representative ERK5 immunostaining of tissues. (A) A nontumorous liver tissue (chronic hepatitis). The level of ERK5 is elevated in the bile duct (large arrow), bile ductules (arrowheads), and a few small hepatocytes (small arrow). (B, C) Paired tumor (B) and nontumor (C) tissues from one HCC patient, wherein the level of ERK5 is elevated in the tumor compared with the counterpart nontumor tissue. Original magnification, ×400.

features of nontumorous liver tissues (Supp. Info. Table 1).

Downregulation of *MAPK7* Inhibits the Growth of HCC Cells

To investigate the effects of *MAPK7* overexpression on HCC cells, we knocked down its expression using RNAi. In SNU449 cells treated with siRNA targeting *MAPK7*, we observed a decrease in *MAPK7* mRNA and ERK5 protein levels relative to that observed for cells receiving a control siRNA or transfection agent alone (Figs. 5A and 5B). The siRNA-mediated downregulation of *MAPK7* suppressed the growth of SNU449 cells at all time points assayed over a 72-hr period (Fig. 5C). These findings suggest that ERK5 promotes the growth of HCC cells.

ERK5 is Phosphorylated During the G2/M Phases of the Cell Cycle

To help elucidate the underlying mechanism by which ERK5 regulates cellular proliferation we investigated the role of ERK5 in cell cycle progression. SNU449 cells were synchronized at G1/S, early S, or M phases of the cell cycle using a double-thymidine, aphidicolin, or nocodazole block, respectively. We determined the levels of total ERK5 and phosphorylated (active) form of ERK5. Immunoblotting did not show a difference in the level of total ERK5 among the three phases of the cell cycle (Fig. 6A). To detect phosphorylated ERK5, total ERK5 was immunoprecipitated from cell lysates using an anti-ERK5 antibody and then analyzed by immunoblotting using an anti-phospho-ERK5 antibody. Phosphorylated ERK5 was more abundant in cells synchronized at the M phase than in asynchronous cells (Fig. 6B).

We next synchronized SNU449 cells at the G1/S boundary using a double-thymidine block and then released the cells from the block. Using flow cytometry, we confirmed the synchrony of the cell cycle and monitored its progression after removal of thymidine (Fig. 6C). There was no difference in the level of total ERK5 during progression of the cell cycle (Fig. 6D). Expression of phosphorylated ERK was maximal 9 hr after release from the block (Fig. 6E), a time when a large proportion of cells were in the G2/M phase (Fig. 6C). Taken together, these observations indicate that ERK5 is phosphorylated during the G2/M phases of the cell cycle.

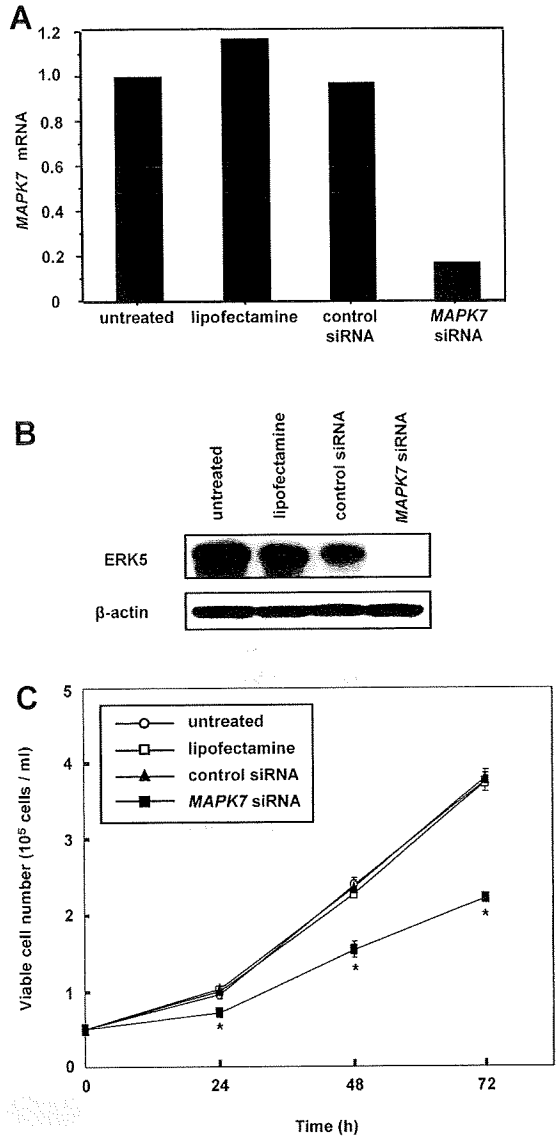

Figure 5. Growth inhibition of SNU449 cells by knockdown of *MAPK7*. A: Relative expression levels of *MAPK7* mRNA as determined by real-time quantitative RT-PCR. SNU449 cells were treated with siRNA targeting *MAPK7*, negative control siRNA, or the transfection agent alone (Lipofectamine), and harvested 48 hr after transfection. Untreated cells were maintained under identical experimental conditions. Results are presented as a ratio between the expression level of *MAPK7* and that of a reference gene (*GAPDH*) to correct for variation in the amount of RNA. Relative expression levels were normalized such that the ratio in untreated cells is 1. B: Levels of ERK5 and β-actin, an internal control, determined by immunoblotting. C: Cell growth was assayed by counting the viable cells at the indicated times after transfection. Each assay was performed in triplicate. Values are represented as the mean ± SD. Differences were analyzed by ANOVA (*$P < 0.01$).

ERK5 Regulates Entry into Mitosis

Our results indicating that ERK5 is activated during the G2/M phases in SNU449 cells suggested that ERK5 may be involved in G2/M progression. To examine whether ERK5 plays a role in mitotic entry, we knocked down *MAPK7*